IEEE Access
Multidisciplinary | Rapid Review | Open Access Journal

Received November 13, 2020, accepted December 5, 2020, date of publication December 9, 2020,
date of current version December 22, 2020.

Digital Object Identifier 10.1109/ACCESS.2020.3043496

Passive Fetal Monitoring by Advanced Signal Processing Methods in Fetal Phonocardiography

RADEK MARTINEK[1], (Member, IEEE), KATERINA BARNOVA[1], RENE JAROS[1], RADANA KAHANKOVA[1], TOMASZ KUPKA[2], MICHAL JEZEWSKI[3], ROBERT CZABANSKI[3], ADAM MATONIA[2], JANUSZ JEZEWSKI[2], (Senior Member, IEEE), AND KRZYSZTOF HOROBA[2]

[1]Department of Cybernetics and Biomedical Engineering, Faculty of Electrical Engineering and Computer Science, VSB—Technical University of Ostrava, 708 00 Ostrava, Czech Republic
[2]Łukasiewicz Research Network, Institute of Medical Technology and Equipment, 54-066 Wrocław, Poland
[3]Department of Cybernetics, Nanotechnology, and Data Processing, Silesian University of Technology, 44-100 Gliwice, Poland

Corresponding author: Rene Jaros (rene.jaros@vsb.cz)

This work was supported in part by the Ministry of Education of the Czech Republic under Project SP2020/156, and in part by the European Regional Development Fund in the Research Centre of Advanced Mechatronic Systems Project, within the Operational Programme Research, Development, and Education, under Project CZ.02.1.01/0.0/0.0/16 019/0000867.

ABSTRACT Fetal phonocardiography (fPCG) is a non-invasive technique for detection of fetal heart sounds (fHSs), murmurs and vibrations. This acoustic recording is passive and provides an alternative low-cost method to ultrasonographic cardiotocography (CTG). Unfortunately, the fPCG signal is often disturbed by the wide range of artifacts that make it difficult to obtain significant diagnostic information from this signal. The study focuses on the filtering of an fPCG signal containing three types of noise (ambient noise, Gaussian noise, and movement artifacts of the mother and the fetus) having different amplitudes. Three advanced signal processing methods: empirical mode decomposition (EMD), ensemble empirical mode decomposition (EEMD), and adaptive wavelet transform (AWT) were tested and compared. The evaluation of the extraction was performed by determining the accuracy of S1 sounds detection and by determining the fetal heart rate (fHR). The evaluation of the effectiveness of the method was performed using signal-to-noise ratio (SNR), mean error of heart interval measurement ($\overline{|\Delta T_i|}$), and the statistical parameters of accuracy (ACC), sensitivity (SE), positive predictive value (PPV), and harmonic mean between SE and PPV (F1). Using the EMD method, ACC $>$ 95% was achieved in 7 out of 12 types and levels of interference with average values of ACC $=$ 88.73%, SE $=$ 91.57%, PPV $=$ 94.80% and F1 $=$ 93.12%. Using the EEMD method, ACC $>$ 95% was achieved in 9 out of 12 types and levels of interference with average values of ACC $=$ 97.49%, SE $=$ 97.89%, PPV $=$ 99.53% and F1 $=$ 98.69%. In this study, the best results were achieved using the AWT method, which provided ACC $>$ 95% in all 12 types and levels of interference with average values of ACC $=$ 99.34%, SE $=$ 99.49%, PPV $=$ 99.85% a F1 $=$ 99.67%.

INDEX TERMS Fetal phonocardiography (fPCG), fetal heart rate (fHR), non-invasive fetal monitoring, empirical mode decomposition (EMD), ensemble empirical mode decomposition (EEMD), adaptive wavelet transform (AWT).

I. INTRODUCTION

Electronic fetal monitoring is an important part of obstetrics, used mainly to prevent fetal hypoxia. Hypoxia is a dangerous condition, and if it is diagnosed, it is necessary to terminate the pregnancy by caesarean section [1]. In clinical practice, a cardiotocography (CTG) method, is used for fetal monitoring. However, fetal monitoring using CTG is burdened with a high degree of disagreement among obstetricians, leading to a high number of unnecessarily performed caesarean sections [2]–[5]. The efforts of scientists are focused on improving alternative methods for

The associate editor coordinating the review of this manuscript and approving it for publication was Chuan Li.

fetal monitoring such as fetal electrocardiography (fECG) [6], [7], fetal magnetocardiography (fMCG) [8], [9] or fetal phonocardiography (fPCG) [10]–[13]. A comparison of the advantages and limitations of techniques for electronic fetal monitoring is summarized in Table 1.

The fPCG method seems to be one of the most promising techniques based on recording fetal acoustic heart sounds (fHSs) during pregnancy. These sounds are generated by opening and closing of the heart valves and blood flow [14]. They can be described as an almost periodic signal with a frequency of 20 to 110 Hz. There are four heart sounds in total to be distinguished, but only the first heart sound (S1) and the second heart sound (S2) are detectable in fPCG signal recordings [15]. The S1 sound is generated by opening and vibrating the bicuspid and tricuspid valves, formed by the onset of systole, i.e. by a sudden rise in pressure. S1 is the longest and loudest sound with low-frequency vibrations, followed by ventricular ejection, which is also characterized by a low-frequency signal. At this stage, blood is expelled into the aorta and pulmonary arteries [16]. The systolic time interval occurring between S1 and S2 sounds is generally shorter than the diastolic one (between S2 and S1) [15]. The S2 sound is generated by vibrations when closing the semilunar valves during the isovolumic relaxation phase of the diastole. Due to the characteristic differences in the valves, it usually has a lower amplitude and shorter duration than S1 [15], [17]. The acoustic fPCG signal generated in this way provides valuable information on heart murmurs and the fetal heart rate (fHR), which is an important indicator of the health and overall well-being of the fetus [18].

The first mention of the potential diagnostic significance of fHSs was described as early as 1820 by a Swiss obstetrician. However, listening to the fetal heart did not become part of clinical practice until 1833, when Evora Kennedy of Dublin published an extensive book to convince doctors to use fPCG for clinical diagnosis [19]. The first examination of fetal heart sounds was conducted by means of placing the ear on the mother's abdominal wall. The improvement occurred in 1917, when the stethoscope was invented by David Hillis, an American obstetrician. The doctors were able to check at least basic information about the fHR, such as the current fHR, arrhythmias or a cardiac arrest [20]. Stethoscopes are still used today, mainly for their low cost, unlimited life, and independence of power supply. The progress in science and technology has enabled the development of an electronic stethoscope that converts acoustic waves detected from the mother's abdomen into electrical signals. These signals are amplified and digitized in the internal circuits, the ambient interference is eliminated, and the sound energy is optimized for listening at different frequencies [21], [22].

Making a high-quality recording is essential for its further processing and accurate determination of the fHR, therefore, great attention is paid to the development of sensors for obtaining an fPCG signal with the highest possible signal-to-noise ratio (SNR). The simplest, but also the least effective way to detect sound, is based on placing a microphone on the surface of the body [22], [23]. Another method involves placing a piezoelectric crystal in contact with the membrane [22], [24]–[26]. Furthermore, four separate piezoelectric vibration sensors for recording abdominal audio signals were developed in [27]. The passive sensor based on the principle of induction allowing long-term observation of fetal movements and sounds was described in [28]. The authors of study [29] designed a non-invasive fiber-optic sensor and an adaptive signal processing system, which could be used for non-invasive fHR monitoring in the future.

It is the complete non-invasiveness of this technique that makes the fPCG a very useful tool suitable for use in clinical practice. Other advantages of this approach include the low cost of the examination, and moreover, both the mother and the fetus are not exposed to any kind of radiation, as in the case of CTG. The CTG method uses ultrasound radiation, which is a potential risk for both the mother and the fetus, thus not allowing long-term monitoring [30].

II. STATE OF THE ART

In addition to the large number of advantages of the fPCG technique mentioned above, it is important to note its limitation, which consists in the presence of interfering signals that are recorded from the abdominal area of the mother together with the useful fetal signal. The most significant types of interference include ambient noise, door closing, speech, breathing or movement artifacts, cough, organ sounds, and other [10], [31]. When examining with a stethoscope, it is necessary to pay attention to its correct location and minimizing the ambient noise, so that the fHSs are clearly audible. Possible artifacts can then be eliminated by selecting a suitable filtration method and its optimal settings.

A. METHODS FOR FETAL PCG EXTRACTION

In order to obtain a high-quality fPCG signal, a number of studies dealing with filtration methods for fPCG extraction have been presented in the past few years. However, in addition to an effective filtration, it is also necessary to choose an appropriate algorithm that can accurately detect the fHSs. Some authors deal with the detection of S1 and S2 sounds and some with the S1 only, both approaches are sufficient for the determination of the fHR. Moreover, some focus on signal segmentation, and, besides S1 and S2, they detect systolic and diastolic intervals. The subsequent analysis of these fPCG signal elements enables obtaining important information and differentiates the fPCG signals into abnormal or normal [18]. Some commonly used techniques for fPCG signals extraction are summarized in this subchapter.

- A combination of adaptive correlation and signal power was used in the study [11]. The accuracy of the method was compared with simultaneously measured ultrasound recordings. The test results showed the possibility of implementing the method in a portable device for continuous monitoring of fHR.
- The authors of study [32] implemented simplified spectral subtraction to remove unwanted noise occurring

TABLE 1. Comparison of techniques for electronic fetal monitoring.

Method	Technical specification	Advantages	Limitations
CTG	Ultrasound transducer and uterine contraction pressure transducer	Noninvasive Measurement of uterine contractions	Ultrasound radiation Sensitivity to maternal movements Sensitivity to sensor location Requires skilled specialist
fMCG	Detection of magnetic fields of the heart using highly sensitive superconducting quantum interference device (SQUID) sensors	Noninvasive High SNR Morphological analysis of the signal	Expensive Requires a shielded room Requires skilled specialist
Invasive fECG	Fetal scalp electrode in the form of a spiral wire	High SNR Morphological analysis of the signal	Infection risks Usability only during delivery
Noninvasive fECG	Standard ECG electrodes	Noninvasive Cheap Continuous monitoring of fHR	Low SNR Difficult to perform a morphological analysis of the signal
fPCG	Vibration or sound converter into an electrical signal; microphones or pressure transducers	Noninvasive Cheap Fully passive Continuous monitoring of fHR Information on heart murmurs	Low SNR Sensitivity to sensor location Sensitivity to ambient noise

in the fPCG signal. However, the performance of this method was not as promising as when using CTG. The authors therefore recommend the use of this technique only as a supplementary tool.

- Wavelet transform (WT), which was presented, for example, in studies [13], [33]–[40], is a frequently tested and very effective method. The results in these studies proved that WT can very effectively suppress noise with the optimal setting of this method. Combining this algorithm with other filtration methods will further increase the effectiveness of filtration. Many authors, therefore, believe that monitoring devices based on this algorithm belong to the most promising techniques for continuous fHR monitoring.
- In studies [10], [41], [42], a method based on the decomposition of the input signal into intrinsic mode functions (IMFs), which is called empirical mode decomposition (EMD), was tested. As with the WT, its optimal setting is crucial for this method. According to the results achieved, this method can very well suppress especially low-frequency interference.
- Independent component analysis (ICA) and principal component analysis (PCA) are well-known and widely used methods based on the principle of blind source separation (BSS). The PCA was tested in study [43] and both of these methods were then investigated, for example, in study [44], where the experiments were performed on synthetic signals. Both methods, ICA and PCA, achieved very good results for SNR improvement and fHR determination, but higher accuracy was achieved using the ICA method.
- Adaptive filters, which are self-learning filters changing their parameters depending on the change in the parameters of the input signal, are also very popular. These types of filters allow filtering interference from the useful signal if it changes its parameters over time or its parameters are not known in advance. The least mean square (LMS), normalized least mean square (NLMS) and recursive least square (RLS) filters were presented in [45]. The LMS and NLMS algorithms were also tested in study [29]. The testing was performed on synthetic recordings and the experiments showed that the NLMS algorithm achieved better results in determining the fHR according to the sensitivity and positive predictive value parameters, while the LMS algorithm achieved better results according to the SNR and root mean square error RMSE) parameters.
- The authors of study [12] successfully extracted source signals from noisy single-channel abdominal recordings. Firstly, an appropriate matrix of delays was constructed, then multiple independent components were calculated, and, finally, the components were projected back onto the measurement space and grouped using K-means method. Three single-channel abdominal fPCG signals having a length of 3 to 5 minutes were used. The signals were obtained from pregnant women between 36 and 40 weeks of gestation. The results of the experiments proved high quality filtration of fPCG signals.
- In study [46], a method based on single-channel separation consisting of three steps was described. The proposed methodology combines the EMD method, singular value decomposition (SVD) and efficient version of fast independent component analysis (EFICA). Again, very good results were obtained in filtering the fPCG signals.

B. DETECTION OF HEART SOUNDS

After signal filtering, it is possible to detect the fHSs in order to extract useful information. A relatively large number of studies are currently being focused on the development of methods for the correct S1 and S2 detection in the classical PCG signal. Fortunately, most of these methods are

also suitable for the fHSs detection in the fPCG recording. In this section a brief review of the literature is presented. An extensive overview of techniques for localizing HSs can be found for example, in studies [18], [47].

- Autocorrelation, being dealt with in study [40], is, for example, one of the oldest approaches used to detect S1 sounds. Unfortunately, this method was not effective for signals with high noise levels. To achieve better results, other methods (WT, matching pursuit, or model-based individual correlation) were combined with autocorrelation. Using these combined approaches, accurate detection of S1 sounds can be achieved.
- The authors of study [48] used an S1 and S2 sound detection and classification algorithm consisting of 4 steps. In the first step, all sounds were localized using optimized S-transform, then the detection of S1 and S2 was performed based on Shannon energy of S-transform, followed by feature extraction using singular value decomposition (SVD) and classification using artificial neural network (ANN). This approach was effective on recordings containing noise and murmurs.
- In study [49], a very frequently used duration-dependent hidden Markov model (DHMM), which was further developed in study [50], was used for the detection of HSs along with systolic and diastolic intervals. This approach was based on the identification of the most probable sequence of HSs based on the duration of the events and the amplitude of the signal envelope. The testing, which was performed on real PCG recordings from adult patients, showed that the DHMM method is suitable for segmentation of real clinical PCG recordings.
- The authors of study [51] proposed an algorithm that identifies HSs using a method based on Gaussian regression. The results of the experiments proved that this algorithm is suitable for S1 and S2 sounds detection and the extraction of cardiac murmurs.
- In study [52], an algorithm combining several approaches was used for the detection and subsequent classification of HSs and murmurs. First, the WT method, which decomposed the input signal so that HSs and heart murmur subbands could be detected, was applied. Subsequently, the Hilbert phase envelope determination was performed to identify the boundaries of HSs segments. The classification of HSs and heart murmurs was then performed on the basis of the temporal features.
- Study [53] presents a method for automatic S1 and S2 sounds detection using the ensemble empirical mode decomposition EEMD) method combined with kurtosis features. The method was tested on real recordings and the experiments provided very promising results.
- The authors of studies [54], [55] identified S1 and S2 sounds by means of a signal envelope detection algorithm using Shannon energy. The peaks were identified using the local maximum and minimum search function. The algorithm was able to detect HSs very effectively.
- In study [56], the detection of S1 and S2 sounds using a combination of frequency filtering, energy detection, and interval regulation was presented. The proposed approach allowed for the localization of HSs with higher accuracy than using the Hilbert transform-based method. The algorithm could thus become very useful for peak detection in various applications.
- Studies that focus on the localization and recognition of fHSs in fPCG signals include also the work [57], where an envelope detector using Hilbert transform and interrelated supplementary processes were used for S1 and S2 detection. Subsequently, thresholding was applied and the envelope was converted to rectangular pulses. Detection of S1 and S2 sounds was based on the knowledge of systolic and diastolic period lengths.
- Study [24] was based on a similar principle, but squared value of the Shannon energy was selected to detect the signal envelope. The envelope was then divided into 40 ms long segments and the fHSs contained in them were identified as local maxima.
- In studies [38], [58], an iterative PCG delineator was used to detect fHSs in fPCG signals. This threshold-based detector identified both S1 and S2 sounds. The results of the experiments showed that the algorithm is able to effectively determine the location, and, moreover, the morphology of the fHSs.
- The authors of study [35] used a combination of WT and fractal dimension methods to identify fHSs. The fractal dimension method was used as a means of detecting the most important WT coefficients that correspond to the fHSs in the WT domain, and very promising results were obtained in the experiments.

From the aforementioned examples, it is obvious that many authors are involved in the extraction and analysis of classical PCG signals, but only a fraction of studies focus on processing of fPCG signals. In addition, different authors use different recordings and different evaluation parameters for testing, and an objective comparison of the performance of the methods presented is almost impossible. The aim of this study is to make an objective, comprehensive comparison of three advanced signal processing methods in terms of S1 sounds detection and fHR determination.

III. MATERIAL AND METHODS

This section describes the methods that have been tested for the purpose of filtering fPCG signals. Methods, which, according to the literature review, have a high potential to effectively filter the noisy fPCG signals, have been selected. They include empirical mode decomposition (EMD), ensemble empirical mode decomposition (EEMD), and adaptive wavelet transform (AWT). Next, the types of interference that were added to the reference signal and subsequently filtered, are described. The chapter also describes statistical parameters that were used to determine the effectiveness of the filtration method in S1 sounds detection, and procedures used to compare the accuracy in determining the fHR.

A. EMPIRICAL MODE DECOMPOSITION

Empirical mode decomposition (EMD) is a signal processing technique that is able to decompose any non-stationary and non-linear signal into oscillating components. These bandlimited components are also called intrinsic mode functions (IMFs) [46], [59]. Each IMF must comply with two basic conditions. First, the number of extrema and the number of zero crossings must be the same or may differ by one at most. Second, at any point, the mean value of the envelopes defined by the local maxima and the envelopes defined by the local minima is zero [46], [60]. The algorithm is iterative and can be described in the following steps [46], [59]–[61]:

1) The upper and lower envelopes, respectively of the local maxima and minima, are estimated using a cubic spline interpolation.
2) The mean $m(t)$ of the two envelopes is subtracted from the original signal $s(t)$.

$$e_1(t) = s(t) - m(t). \tag{1}$$

3) If $e_1(t)$ meets both of the aforementioned conditions, it is denoted as IMF1. If not, steps 1. and 2. are repeated until the first IMF is obtained.
4) Subsequently, a residue $r_i(t)$ is defined by subtracting $e_1(t)$ from the input signal $s(t)$.

$$r_i(t) = s(t) - e_1(t). \tag{2}$$

5) To obtain subsequent IMFs, the entire process is repeated, but, instead of the input signal $s(t)$, the residue $r_i(t)$ is used.

The entire process is repeated until the final residue is a monotonic function or a constant. The original signal can be reconstructed by summing all extracted IMFs and the last residue. More detailed description of the method can be found, for example, in [60]–[63]. In [10], [46], [59], [64], the method was tested for the purpose of fPCG filtration.

B. ENSEMBLE EMPIRICAL MODE DECOMPOSITION

The ensemble empirical mode decomposition (EEMD) method was devised as an improved version of the empirical mode decomposition (EMD) procedure. The EMD is very effective, but it is burdened by limitations in the form of so-called *mode mixing* problem [53], [65]. This is a phenomenon in which the EMD is not able to correctly decompose the signal into individual IMFs, resulting in one IMF containing several components of very different frequencies. This problem usually occurs when the original low-frequency signal contains discontinuous and isolated high-frequency oscillations [66], [67]. To prevent this phenomenon, an extended version of this method, termed EEMD, was proposed. With the EEMD, individual IMFs are obtained by averaging the results of several EMD cycles, wherein random white noise with a predefined amplitude is added to the input signal [66]. The EEMD method algorithm can be described in the following steps [53], [66]–[68]:

1) Set the number of ensemble trials N and the standard deviation of the added noise N_{std}.
2) Add a random white noise to the input signal.
3) Decompose the resulting signal into individual IMFs using EMD algorithm.
4) Repeat step 1 and 2 N-times, but with different white noise series each time.
5) Determine the final $IMF_j(t)$ of the EEMD by averaging all IMFs related to N trials.

$$IMF_j(t) = \frac{1}{N}\sum_{i=1}^{N} IMF_{i,j}(t), \tag{3}$$

where j is a number of an IMF scale.

The added white noise leads to the correct decomposition of the signal into IMFs using the EMD method. The final result is the average of a large number of iterations, in which a different white noise is used. By averaging, the white noise is eliminated, and only the resulting signal remains. More detailed information on this method can be found, for example, in [65], [67]–[69]. For the purpose of fPCG processing, the method was tested in study [70], and, for the purpose of PCG processing, it was used in [53], [71].

C. ADAPTIVE WAVELET TRANSFORM

Wavelet transform (WT) is a well performing method of filtering the noise in non-stationary signals. It is also a well-known technique that is used to eliminate the noise in fPCG signals [33]. Unlike the Fourier transform (FT), this advanced signal processing technique can provide good representation of a signal in the time-frequency domain.

After discretization, the discrete wavelet transform (DWT) can be defined as [33], [72]:

$$DWT_\psi(j,k) = \int_{-\infty}^{\infty} s(t)\cdot\psi^*_{j,k}(t)dt, \tag{4}$$

where $\psi^*_{j,k}$ is the wavelet function after dilation and translation.

$$\psi^*_{j,k} = 2^{\frac{j}{2}}\psi(2^j t - k), \tag{5}$$

in which function ψ indicates the maternal wavelet, $\psi_{j,k}$ denotes the daughter wavelet, j is a scale parameter and k is a grid parameter [33]. After applying the WT to the input signal, the wavelet coefficients are obtained, which are then thresholded. Universal thresholds, minimax thresholds, Stein's unbiased risk estimation (SURE), empirical thresholds, etc., are often used to remove the noise from non-stationary signals [73]. In this study, adaptive thresholding was used, i.e. each wavelet coefficient was assigned with a certain threshold value. A moving window with a specified length is used, whereby the threshold responds to changes of the noise power in the signal waveform [74]. Thresholding can be further divided into hard and soft. In the case of hard thresholding, the coefficients below the threshold are replaced by zeros, while, in the case of soft thresholding, the remaining non-zero coefficients are shifted towards zero by

the size of the threshold [73], [74]. Finally, an inverse discrete wavelet transform (IDWT) was used to reconstruct the filtered fPCG signal [33]. Much literature deals with the issue of WT. A detailed information can be found, for example, in [72], [75]–[79], while in [13], [33], [33]–[35], [37], [38] the WT application for the purpose of fPCG processing was discussed.

D. REFERENCE SIGNAL AND NOISE

Recordings on which the algorithms are tested and evaluated form an essential part of the development of methods on fPCG processing. Unfortunately, the number of databases containing fPCG recordings is still very limited. Currently, only two databases containing clinical data and one database containing synthetic data are available. These databases can be found in the *PhysioBank* archive [80]. The databases with real data include the *Fetal PCGs database* [81] and *Shiraz University Fetal Heart Sounds Database* [82], whereas synthetic fPCG data can be obtained from the *Simulated Fetal PCGs database*. Simulation software generating fPCG signals is able to imitate physiological and pathological conditions of the fetus by simply modifying some system parameters [16]. The disadvantage of real recordings, compared to synthetic ones, is the absence of a reference which the filtered signal could be compared with. Therefore, a 300 second synthetic signal (a reference) with a sampling frequency of 1000 Hz and an average fHR of 140 bpm was used in this study. The signal corresponds to the ideal fPCG with a gestational age of 40 weeks. Three types of interference having different amplitudes were added to the reference recording, which were subsequently filtered by the selected methods. An example of a reference signal and all three types of interference is shown in Fig. 1. The created and used dataset can be found in `https://dx.doi.org/10.21227/tgvb-rw67` [83]. The considered classes of interference are:

- *Ambient noise* - this is any noise from the surroundings. It occurs commonly when recording the fPCG. Its spectrum includes frequencies from 10 Hz.
- *White Gaussian noise* - a random signal with the same power in any band of the same width.
- *Maternal and fetal movement artifacts* - a noise caused by muscle movement or breathing. They occur at low frequencies, usually up to 100 Hz.

Fig. 2 shows a comparison of the waveforms and frequency spectra of a reference and noisy fPCG signals. Each sub-figure contains one type of interference with different intensities. Of course, the added noise signals have lower SNR than the reference fPCG signal. The level of SNR with the type of noise is listed in Table 3.

The interference used was created using available fPCG databases, see [16], [80]–[82], [84]. The fPCG signal can be expressed by the following expression:

$$x(t) = s(t) + n(t), \tag{6}$$

where $s(t)$ represents the ideal physiological fPCG signal and $n(t)$ represents superimposed interferences of various type

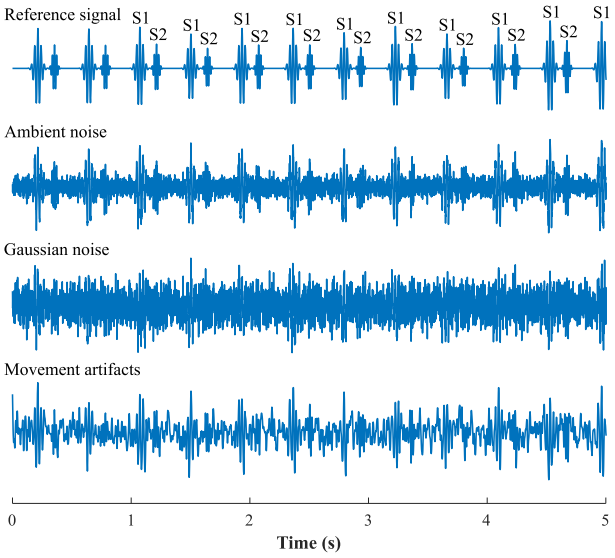

FIGURE 1. An example of a reference signal and all three types of interference (ambient noise, Gaussian noise, and movement artifacts).

and SNR level. Fig. 2 show these signals in time and frequency spectra, respectively. As mentioned above, it is impossible to acquire an ideal fPCG. For these reasons, the $n(t)$ signal reflects artifacts occurring in the fPCG signal including fetal movements and respiration, physiological sounds caused by maternal body (e.g. heart sounds, respiratory activity, muscle contractions). Table 2 represents a summary of the interference we may encounter when monitoring fPCG.

Noise from the surrounding environment caused by speech and other sounds sums up in so-called background noise. Sensor noise is caused by quantization noise of the recording device. Both of these types of interference (SBN - sensor and background noise) are random white Gaussian wideband signals. They occur at all frequencies throughout the recording and lead to a change in the mean and deviation of the signal obtained.

Significant fetal movements usually last longer than 4 s, which include change of the fetal position and orientation; movements lasting from 1 to 3 s are caused simply by moving the limb or head. The frequency range of these movements should be in the range 0–25 Hz. Although the fetus does not have functional lungs until birth and receives nutrients and oxygen through the placenta, the lungs produce respiratory movements. Fetal respiration or hiccups fall between short movements lasting less than 1.5 s and fall in the frequency band 0.3–1.5 Hz. Uterine contractions, breathing or digestive sounds of the mother are low-frequency signals that create amniotic fluid vibrations and thus interference when sensing the fPCG signal. The frequency, intensity and duration of uterine contractions are highly related to the week of pregnancy. In general, they occur 2–5 times every 10 minutes and their duration is variable, from 15 to 70 s. Maternal respiration occurs in the 0.2–2.5 Hz band and has a relatively higher amplitude compared to fHS and sensor and ambient noise. Respiration produces isoline fluctuations that overlap with

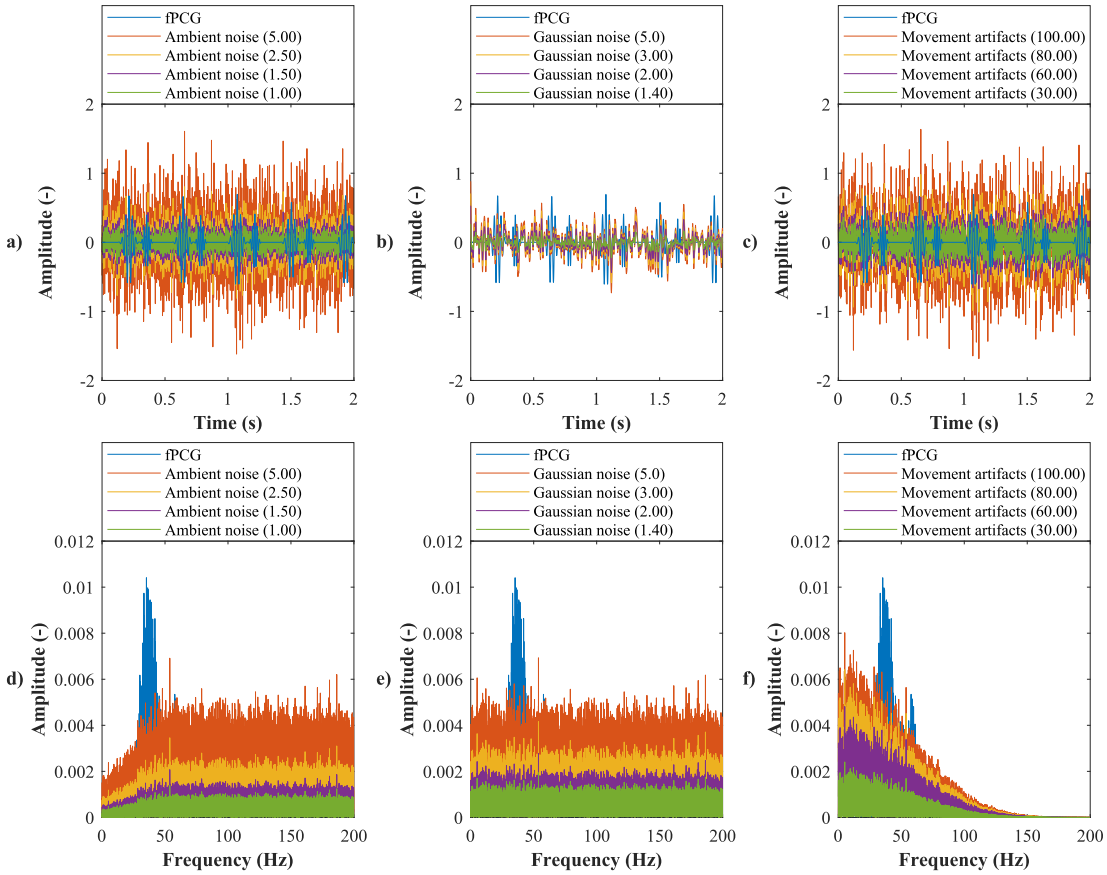

FIGURE 2. Waveforms and frequency spectrum of fPCG signal (blue) and noise of different intensities and types: a) and d) ambient noise, b) and e) Gaussian noise and c) and f) movement artifacts.

TABLE 2. Overview of components in the fPCG signal. fHS - fetal heart sounds, fM - fetal movements, fR - fetal respiration, mHS - maternal heart sounds, mR - maternal respiration, UC - uterine contractions, mM - maternal movements, PLI - powerline interference, RN - reverberation noise, SBN - sensor and background noise.

Component	Frequency band (Hz)	Duration (s)	Relative amplitude	Effect on fPCG recording
fHS	15–110	Continuous	SBN, fR, < fHS < mHS, mR, RN, FM	- useful signal
fM a hiccups	0–25	1–3	SBN < fM < mHS, mR, fR, mDS, fHS	- random impulses in fPCG
fR	0.3–1.5	Continuous	SBN < fR < fHS, mHS, mR, RN, fM	- baseline wander - fHR variations
mHS	10–40	Continuous	SBN, fR, fM, mR < mHS < RN	- overlap with fHS in time and frequency domain, - unwanted morphological changes in fPCG
mR	0.2–0.5	Continuous	SBN, fR, fHS, fM < mR < mHS, RN	- baseline wander - fHR variations
UC	0.2–0.5	15–60	–	–
mM	0–100	Variable	SBN, fR, fHS, fM, mHS < mM, RN	- produces RN
PLI	50/60	Continuous	–	- unwanted morphological changes in fPCG
RN	–	–	SBN, fR,fHS, fM, mHS < mM, RN	- random impulses in fPCG decreasing SNR
SBN	Broadband	Continuous	SBN < fR, fHS, mHS, mM, RN	- change in mean value and variation of fPCG

fHR and fetal respiration in the frequency domain. There is not enough information about digestive sounds and their influence on the fPCG signal in the literature. All these types of interference can be likened to random white Gaussian noise and their frequency band is 0.2–0.5 Hz. Maternal heart sounds can be classified as frequencies of 10–40 Hz. Maternal movements lead to random impulses with high amplitude creating echo noise. Table 2 shows overview of components in the fPCG signal.

Signals $n(t)$ defined by Eq. (6) were modeled on the basis of [15], i.e. modeling the sounds of the gastrointestinal tract, maternal respiration and fetal movements were performed by passing white noise through a fifth-order Butterworth low-pass filter with a cut-off frequency of 25 Hz. The resulting signal was a low amplitude band signal in the range of 0 to 25 Hz. The background noise is modeled by a fifth-order Butterworth high-pass filter with a cut-off frequency of 100 Hz.

TABLE 3. Settings of EMD, EEMD, and AWT algorithms.

Type of artifacts	Interference amplitude (-)	SNR of signal with noise (dB)	EMD	EEMD			AWT		
			IMFs	N	N_{std}	IMFs	Wavelet type	Thresholding	Number of decomposition levels
Ambient noise	1.00	-1.16	3+4+5	10	0.3	4	db4	hard	3
	1.50	-2.27	4	10	0.2	4	db4	hard	3
	2.50	-4.63	4	30	0.2	4+5	sym4	soft	3
	5.00	-9.36	4	30	0.2	4+5	db4	soft	3
Gaussian noise	1.40	-2.12	4	10	0.2	4+5	sym4	hard	3
	2.00	-3.58	4	10	0.2	4+5	sym4	soft	3
	3.00	-5.89	4	30	0.1	4+5	db4	soft	3
	5.00	-9.55	5	30	0.1	4+5	db4	soft	3
Movement artifacts	30.00	-0.50	2	10	0.3	3+4+5	sym4	hard	3
	60.00	-1.74	2	10	0.2	3+4	sym4	hard	3
	80.00	-2.73	2	30	0.2	3+4	db4	soft	3
	100.00	-3.74	2	30	0.1	3+4	db4	soft	3

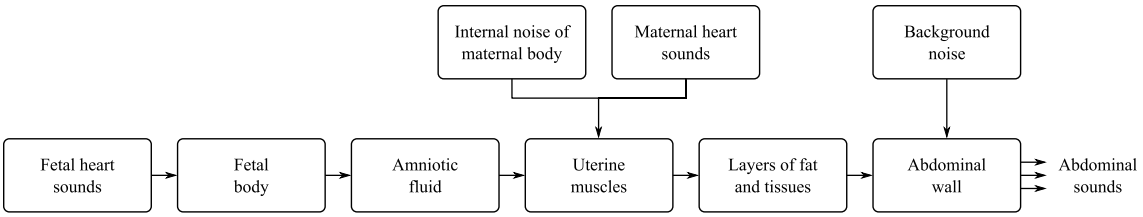

FIGURE 3. Block diagram of heart sound transmission.

Maternal movements are modeled as random pulses with a fixed amplitude lasting 0.5 to 1.5 s, see more details in [15]. This fPCG signal model is a direct linear superposition of fHS, mHS and noise, see Eq. (6). The first type of interference used for the performed experiments is Gaussian noise with different noise levels (according to the used constant 1.4; 2; 3 and 5 corresponding to the SNR value in dB), see Fig. 2 and Table 3. The second type of interference is the so-called Movement artifacts, again with different noise levels (according to the used constant 30; 60; 80; 100 corresponding to the SNR value in dB), see Fig. 2 and Table 3. This signal reflects the activity of the muscles of the fetus and mother, including respiration. The last type of interference used is Ambient noise with different noise levels (according to the used constant 1; 1.5; 2.5 and 5 corresponding to the SNR value in dB), see Fig. 2 and Table 3. Fig. 3 shows block diagram of heart sound transmission.

E. EVALUATION METHODS

The filtered fPCG signal can be evaluated subjectively or objectively. The subjective evaluation can be performed by comparing the waveforms of the filtered signal with the ideal reference signal. In the case of fPCG, it can also be evaluated by listening to the signals. SNR and mean error of heart interval measurement $\overline{|\Delta T_i|}$, statistical evaluation of the accuracy of S1 sounds detection and fHR determination were used for the objective evaluation. The fHR determination accuracy was ensured by plotting fHR traces and Bland-Altman plots. The quality indices that are used to verify the proposed method are the following:

- *Signal-to-noise ratio* - the SNR parameter is used to evaluate the ratio between the useful signal and the noise. The unit for SNR is the decibel (dB). By subtracting the input SNR (SNR_{in}) from the output (SNR_{out}), the SNR increase is calculated, making it possible to find out the signal improvement after filtering. The following equations are used to determine the SNR_{in} and SNR_{out} [44]:

$$SNR_{in} = 10\log_{10}\frac{\sum_{m=1}^{M-1}(fPCG_{ref}(m))^2}{\sum_{m=1}^{M-1}(fPCG_{in}(m) - fPCG_{ref}(m))^2}, \tag{7}$$

$$SNR_{out} = 10\log_{10}\frac{\sum_{m=1}^{M-1}(fPCG_{ref}(m))^2}{\sum_{m=1}^{M-1}(fPCG_{filt}(m) - fPCG_{ref}(m))^2}, \tag{8}$$

where M is the number of samples of the reference signal ($fPCG_{ref}$), the input signal containing interference ($fPCG_{in}$) and the signal after filtering using the specific method ($fPCG_{filt}$).

- *Detection of S1 heart sounds* - accurate detection of S1 sounds (corresponding to the R peaks in the fetal electrocardiography signal) is crucial for the fHR determination. The detection was performed using the Pan-Tompkins algorithm. First, the noise cancellation is performed, then the signal is derived by a derivative filter, followed by squaring, and moving window integration. Subsequently, the Pan-Tompkins decision rule, using adaptive thresholding, is applied. Thresholding

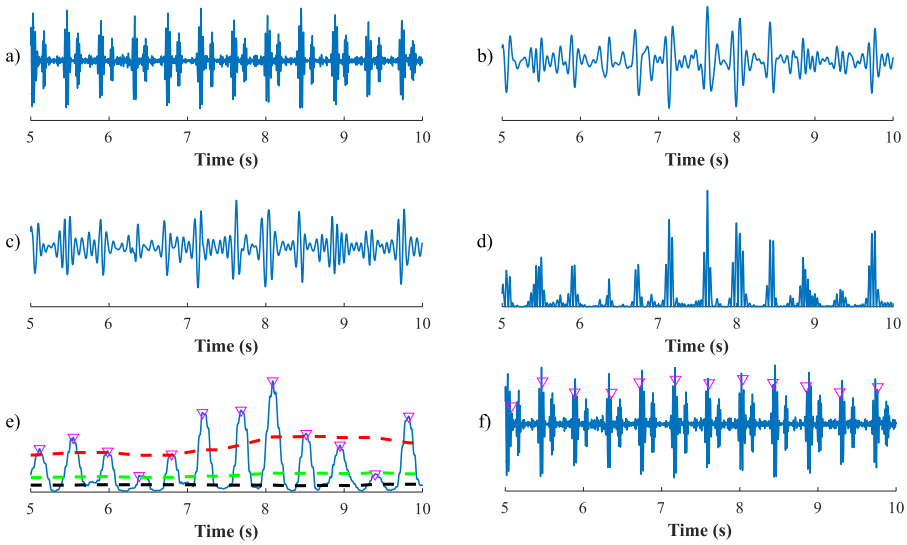

FIGURE 4. Steps of S1 sounds detection using the Pan-Tompkins algorithm: a) input signal, b) signal filtration using a band-pass filter, c) signal filtration using a derivative filter, d) filtered signal is squared to enhance the dominant peaks, e) application of moving averages with detected S1 sounds (red line indicates the signal level, green line indicates the adaptive threshold, black line indicates the noise level), and f) output signal with detected S1 sounds.

determines whether the detector has detected S1 sound or a noise. If S1 is mistakenly considered to be a noise and the next S1 is not detected for a long time, then, a search for the S1 related signal peak is performed, wherein the 166% limit of the average of the last S1–S1 interval. The occurrence of the missing S1 is then assumed at the highest peak in the interval. If S1 is detected, it is not possible for another one to be detected after another 200 ms, due to the refractory period [85]. A detailed description of the algorithm can be found in many references [85]–[87]. An example of S1 sounds detection using Pan-Tompkins algorithm is shown in Fig. 4.

The quality of S1 sounds detection was evaluated using the reference recording. A true positive (TP) assessment was defined as a correctly detected S1 sound, which was determined 50 ms before or 50 ms after the corresponding S1 sound in the reference recording. The assumed interval was inspired by study [88]. A false positive (FP) was defined as a detected, but non-existent S1 sound, while a false negative (FN) is an existing S1 sound which was not detected. Using TP, FP and FN values, it was possible to further determine the accuracy (ACC), the sensitivity (SE), the positive predictive value (PPV), and F1 score [10], [88]:

$$ACC = \frac{TP}{TP + FP + FN} \cdot 100, \tag{9}$$

$$Se = \frac{TP}{TP + FN} \cdot 100, \tag{10}$$

$$PPV = \frac{TP}{TP + FP} \cdot 100, \tag{11}$$

$$F1 = \frac{2 \cdot TP}{2 \cdot TP + FP + FN} \cdot 100. \tag{12}$$

- *Fetal heart rate determination* - the heart rate can be obtained from the fPCG signal using the time intervals between S1 sounds. The fHR traces, which were created by applying the moving averages for the values obtained by the filtration method and for the values of the reference recording, were used for the graphical representation of the fHR. When applying the moving averages, the best results were achieved with a 30-sample window. Furthermore, Bland-Altman plots, which are widely used to evaluate two methods of clinical measurement, were applied for the comparison. Using Bland-Altman plots, systematic differences between the measurements or possible outliers can be identified. The vertical axis shows the difference between paired values, while the horizontal axis shows the arithmetic mean of these values. The middle horizontal line indicates the mean μ of all differences, and, based on this line, a 95% confidence interval, which lies in the interval $\mu \pm 1.96\sigma$, is plotted [89].
- *Mean error of heart interval measurement* $\overline{|\Delta T_i|}$ - this parameter is defined as the mean value of the measurement error $|\Delta T_i|$, which is defined as the absolute value of heart interval differences ΔT_i between the filtered and reference signal:

$$|\Delta T_i| = |T_{i\_filt} - T_{i\_ref}|, \tag{13}$$

where T_{i_filt} is value of the i-th interval determined for the filtered signal and T_{i_ref} is value of the i-th interval determined for the reference signal, the unit is millisecond (ms) [90].

F. ALGORITHMS SETTINGS

To achieve the best possible results, the optimal setting of the parameters of the filtration methods was crucial. For all

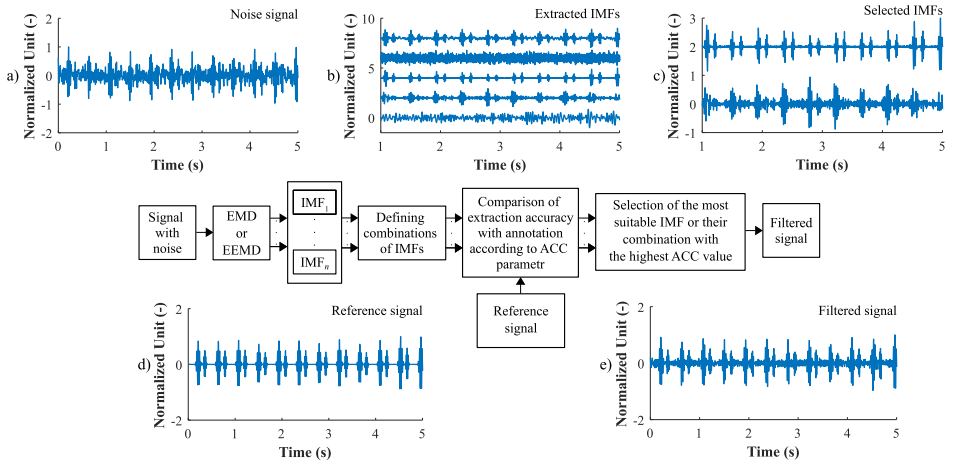

FIGURE 5. Scheme of the algorithm for comparing various combinations of IMFs and selecting the optimal one. The combination that achieved the highest accuracy according to the ACC parameter compared to the reference signal was selected. Examples of a) input signal with noise, b) first five IMFs extracted using EMD or EEMD algorithm, c) selected the most suitable IMFs, d) reference signal and e) resulting filtered signal generated by summing the most suitable IMFs are also presented.

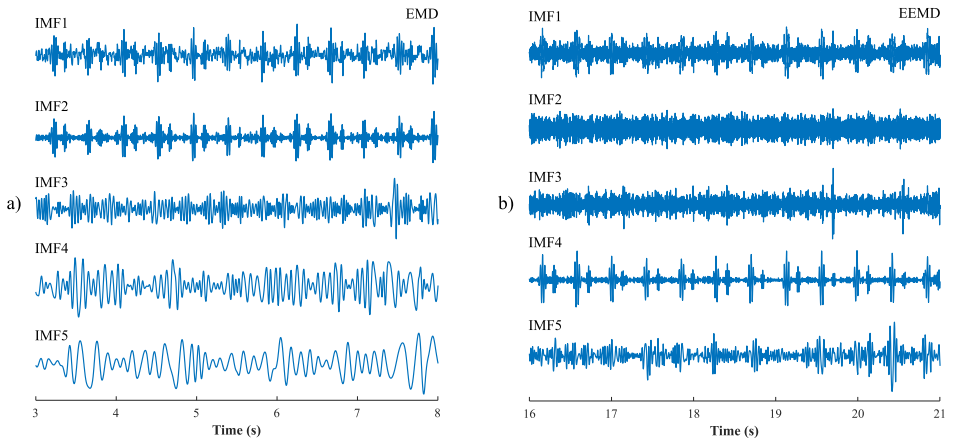

FIGURE 6. Decomposition a) using the EMD method (example of the first 5 IMFs) when filtering movement artifacts multiplied by the interference amplitude of 60 and b) using the EEMD method (example of the first 5 IMFs) when filtering ambient noise multiplied by the interference amplitude of 1.50.

the methods, all parameters were selected based on the automated algorithm comparing the individual combinations of the parameters set. Using this algorithm, the most suitable IMFs were also selected for the EMD and EEMD methods. The output signals generated based on the parameters set or combination of IMFs were compared with a reference signal and evaluated based on the ACC parameter. A combination of parameters or IMFs whose output signal achieved the highest accuracy according to the ACC parameter was selected. The settings of the parameters of the EMD (IMFs combination), EEMD (IMFs combination, N, and N_{std}), AWT (wavelet type, number of decomposition levels, hard or soft thresholding) methods providing the highest value of ACC are shown in Table 3.

1) EMD - the EMD method was based on the decomposition of the input signal into 19 simpler signals called IMFs. The total number of extracted IMFs depends on the signal to be processed. The decomposition process ends when the IMF cannot be extracted. This is a state where the signal is a constant or a monotonic function. Subsequently, the most suitable IMFs were selected using an automated algorithm (as described above) and summed to create a filtered fPCG. Fig. 5 shows a block diagram of automated algorithm for selecting the most suitable combination of IMFs for both EMD and EEMD algorithms. An example of the first five IMFs extracted using EMD is presented in Fig. 6.
2) EEMD - the EEMD method was based on a similar principle as EMD but extracted a total of only 15 IMFs before reaching the stopping criterion. Further, it was also necessary to select the best performing IMFs that were used to obtain the filtered signal, but in addition it was necessary to find the optimal setting of the standard deviation of the added noise series N_{std} and

TABLE 4. Statistical evaluation of the S1 detection quality using the EMD method when filtering ambient noise, Gaussian noise, and movement artifacts of the mother and the fetus.

Type of interference	Interference amplitude (-)	SNR of signal with noise (dB)	Number of S1 in reference	TP	FP	FN	ACC (%)	SE (%)	PPV (%)	F1 (%)	SNR impr. (dB)	$\overline{\lvert\Delta T_i\rvert}$ (ms)
Ambient noise	1.00	-1.16	680	680	0	0	100.00	100.00	100.00	100.00	8.06	0.99
	1.50	-2.27	680	666	2	14	97.65	97.94	99.70	98.81	11.98	32.86
	2.50	-4.63	680	638	17	42	91.54	93.82	97.41	95.58	14.60	64.86
	5.00	-9.36	680	405	190	275	46.55	59.56	68.07	63.53	16.88	213.63
Gaussian noise	1.40	-2.12	680	661	3	19	96.78	97.21	99.55	98.36	11.44	39.44
	2.00	-3.58	680	660	4	20	96.49	97.06	99.40	98.22	14.41	41.37
	3.00	-5.89	680	588	40	92	81.67	86.47	93.63	89.91	15.52	111.30
	5.00	-9.55	680	506	102	174	64.71	74.41	83.22	78.57	21.35	162.39
Movement artifacts	30.00	-0.50	680	680	0	0	100.00	100.00	100.00	100.00	7.14	1.00
	60.00	-1.74	680	678	1	2	99.56	99.71	99.85	99.78	8.30	9.57
	80.00	-2.73	680	670	5	10	97.81	98.53	99.26	98.89	8.57	23.90
	100.00	-3.74	680	640	16	40	91.95	94.12	97.56	95.81	8.61	61.75

the number of ensemble trials N. The most suitable combination of parameters set and combinations of IMFs was also found using an automated algorithm, see Fig. 5. An example of the first five IMFs extracted using EEMD is presented in Fig. 6.

3) AWT - when filtering using the AWT method, optimal settings of type and width of the maternal wavelet and the suitable level of decomposition were crucial. In this study, *symlet* and *Daubechies* wavelets were tested. These wavelet types have a shape similar to the fHSs and their energy and frequency spectrum is similar to the spectrum of the fPCG signal. In addition, according to the literature review, they achieve very good results. The most suitable wavelet width, the number of decomposition levels and the type of thresholding were again selected based on an automated algorithm. The width of the wavelets was tested in the range 1 to 20 with step of 1, the number of decomposition levels was tested in the range 1 to 10 with step of 1, and soft and hard types of thresholding. For all types of interference, it was observed that hard thresholding was more suitable for low noise amplitudes, while soft thresholding worked better with higher noise level.

IV. RESULTS

This chapter provides the results of filtering three types of interference using the methods (EMD, EEMD and AWT) applied individually. The evaluation of the performance was conducted in terms of the success rate of the S1 detection and the fHR determination. A noise-free reference recording was used to compare the filtration effectiveness. The effectiveness was first evaluated according to statistical parameters and, then, by graphical representation of Bland-Altman plots and fHR traces.

A. STATISTICAL EVALUATION

The TP, FP and FN values were first determined for statistical evaluation of the success rate of S1 sounds detection and, based on them, the ACC, SE, PPV and F1 parameters were calculated. The tables show also the value of the SNR increase, $\overline{\lvert\Delta T_i\rvert}$ values, and the type and amplitude of the interference that was added to the reference signal.

- *Empirical mode decomposition* - according to Table 4, it can be noticed that the detection of S1 sounds with the EMD method provides values of ACC and SE above 95% for 7 out of 12 types and levels of interference. The PPV and F1 over 95% were achieved in 9 out of 12 types and levels of interference. In 2 cases, all S1 sounds were correctly recognized and no FP or FN was detected, consequently, all parameters reached the best possible value of 100%. The worst results were obtained with the highest level of the ambient noise (amplitude of 5.00) and the Gaussian noise (also with the highest interference amplitude of 5.00). In both cases, the EMD method was not able to suppress the noise, and low values of ACC (46.55% and 64.71% respectively) were noticed. However, high SNR improvement was observed for all types and levels of interference. For the ambient and the Gaussian noise, lower SNR improvement values were noticed compared to the EEMD and AWT methods, but, for the movement artifacts, higher SNR improvement values were achieved. Low $\overline{\lvert\Delta T_i\rvert}$ values were obtained only at low amplitudes of ambient noise and movement artifacts. Nevertheless, in comparison with the EEMD and AWT, this method achieved the highest $\overline{\lvert\Delta T_i\rvert}$ values and thus the least accurate estimation of heart intervals for the ambient and the Gaussian noise.
- *Ensemble empirical mode decomposition* - based on the presented results (Table 5), it can be seen that the S1 sounds detection with the EEMD method provides values of the ACC and SE parameters over 95% in 9 out of 12 types and levels of interference. Values of PPV parameter of at least 95% were achieved for all types and amplitudes of interference, and the F1 scores exceeded the value of 95% for 11 types and levels of noise. In 5 cases, all S1 sounds were correctly detected and no FP or FN was observed - all quality measures reached the value of 100%. The worst results were noticed for the Gaussian noise with the highest interference (amplitude of 5.00). In this case, the ACC of 89.02% was

TABLE 5. Statistical evaluation of the accuracy of S1 detection using the EEMD method when filtering ambient noise, Gaussian noise, and movement artifacts of the mother and the fetus.

Type of interference	Interference amplitude (-)	SNR of signal with noise (dB)	Number of S1 in reference	TP	FP	FN	ACC (%)	SE (%)	PPV (%)	F1 (%)	SNR impr. (dB)	$\overline{\lvert\Delta T_i\rvert}$ (ms)
Ambient noise	1.00	-1.16	680	680	0	0	100.00	100.00	100.00	100.00	11.53	2.10
	1.50	-2.27	680	680	0	0	100.00	100.00	100.00	100.00	17.67	4.05
	2.50	-4.63	680	679	0	1	99.85	99.85	100.00	99.93	19.36	9.86
	5.00	-9.36	680	635	12	45	91.76	93.38	98.15	95.70	19.71	73.50
Gaussian noise	1.40	-2.12	680	680	0	0	100.00	100.00	100.00	100.00	16.71	3.82
	2.00	-3.58	680	680	0	0	100.00	100.00	100.00	100.00	18.66	5.65
	3.00	-5.89	680	675	1	5	99.12	99.27	99.85	99.56	19.09	18.07
	5.00	-9.55	680	616	12	64	89.02	90.59	98.09	94.19	19.38	99.08
Movement artifacts	30.00	-0.50	680	680	0	0	100.00	100.00	100.00	100.00	1.77	1.73
	60.00	-1.74	680	677	0	3	99.56	99.56	100.00	99.78	7.51	14.18
	80.00	-2.73	680	666	2	14	97.65	97.94	99.70	98.81	7.53	31.90
	100.00	-3.74	680	640	9	40	92.89	94.12	98.61	96.31	7.57	67.16

TABLE 6. Statistical evaluation of the accuracy of S1 detection using the AWT method when filtering ambient noise, Gaussian noise, and movement artifacts of the mother and the fetus.

Type of interference	Interference amplitude (-)	SNR of signal with noise (dB)	Number of S1 in reference	TP	FP	FN	ACC (%)	SE (%)	PPV (%)	F1 (%)	SNR impr. (dB)	$\overline{\lvert\Delta T_i\rvert}$ (ms)
Ambient noise	1.00	-1.16	680	680	0	0	100.00	100.00	100.00	100.00	21.49	0.68
	1.50	-2.27	680	680	0	0	100.00	100.00	100.00	100.00	23.06	0.68
	2.50	-4.63	680	680	0	0	100.00	100.00	100.00	100.00	25.58	3.84
	5.00	-9.36	680	676	1	4	99.27	99.41	99.85	99.63	27.01	19.44
Gaussian noise	1.40	-2.12	680	680	0	0	100.00	100.00	100.00	100.00	19.22	1.05
	2.00	-3.58	680	680	0	0	100.00	100.00	100.00	100.00	20.43	3.45
	3.00	-5.89	680	680	0	0	100.00	100.00	100.00	100.00	21.33	8.44
	5.00	-9.55	680	666	4	14	97.37	97.94	99.40	98.67	21.84	33.56
Movement artifacts	30.00	-0.50	680	680	0	0	100.00	100.00	100.00	100.00	0.85	1.67
	60.00	-1.74	680	678	1	2	99.56	99.71	99.85	99.78	1.33	11.46
	80.00	-2.73	680	676	2	4	99.12	99.41	99.71	99.56	1.51	16.87
	100.00	-3.74	680	662	4	18	96.78	97.35	99.40	98.37	1.64	39.26

achieved. Significant SNR improvement was obtained for all interferences, except for movement artifacts with the amplitude of 30.00. For the ambient and the Gaussian noise, higher SNR improvement was achieved when compared to the EMD method, but lower in comparison to the AWT. For the movement artifacts, lower SNR improvement was achieved when compared to the EMD, but higher comparing to the AWT method. Low $\overline{|\Delta T_i|}$ values were achieved for all types of interference only at low interference amplitudes. In comparison with the EMD and AWT, this method achieved the highest $\overline{|\Delta T_i|}$ values and thus the least accurate estimation of heart intervals for movement artifacts.

- *Adaptive wavelet transform* - it can be noticed that using the AWT method values of all statistical parameters (ACC, SE, PPV and F1 in Table 6) above 95% were achieved for each of the examined tasks. In 7 cases (out of 12), all S1 sounds were correctly identified and there was no FP or FN detection, and the highest possible value of 100% was achieved for all quality measures. High SNR improvement values were obtained for the Gaussian and the ambient noise. For these interferences, higher SNR improvement values were achieved compared to the EMD and EEMD methods. However, for the movement artifacts, lower SNR increase was obtained. Low $\overline{|\Delta T_i|}$ values were achieved for all types of interference only at low interference amplitudes. In comparison with the EMD and EEMD, this method achieved the lowest $\overline{|\Delta T_i|}$ values and thus the most accurate estimation of heart intervals for all classes of inference.

B. VISUAL COMPARISON

In this chapter, the performance of the algorithms will be analyzed from the visual perspective by comparing the waveforms of the signals filtered and the reference recording. Based on the visual comparison, it can be stated that the AWT method was the most effective for the ambient and the Gaussian noise, while the EMD and EEMD were better when filtering the movement artifacts of the mother and the fetus. An example of the filtering outcomes extracted by using all the methods tested for the Gaussian noise (the interference amplitude of 3.00) is shown in Fig. 7. The figure shows clearly that the EMD method suppressed some S1 sounds making their detection impossible, and therefore, the subsequent fHR determination was not successful. Improvements were made by means of the EEMD method, which was able to extract S1 sounds with a sufficiently resolvable amplitude, but still, there are noticeable noise residues in the signal. The best extraction quality was achieved using the AWT method, which was able to extract S1 sounds with a

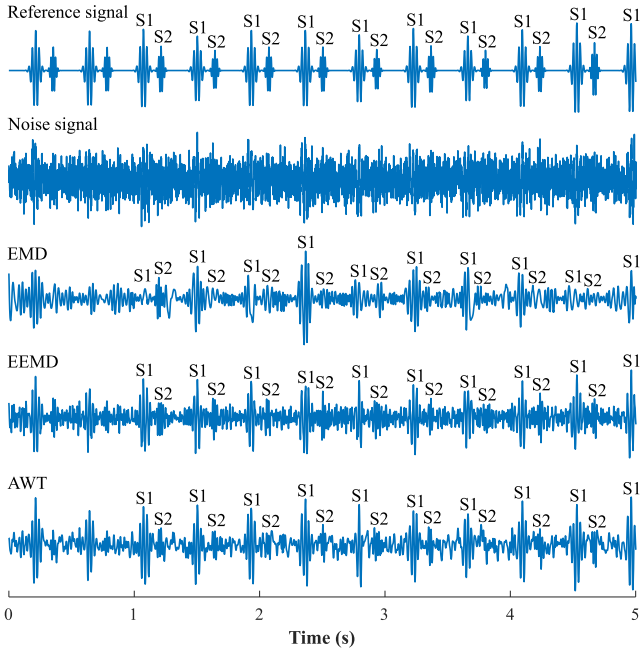

FIGURE 7. An example of the filtering results of the Gaussian noise (the interference amplitude of 3.00) using all the methods tested.

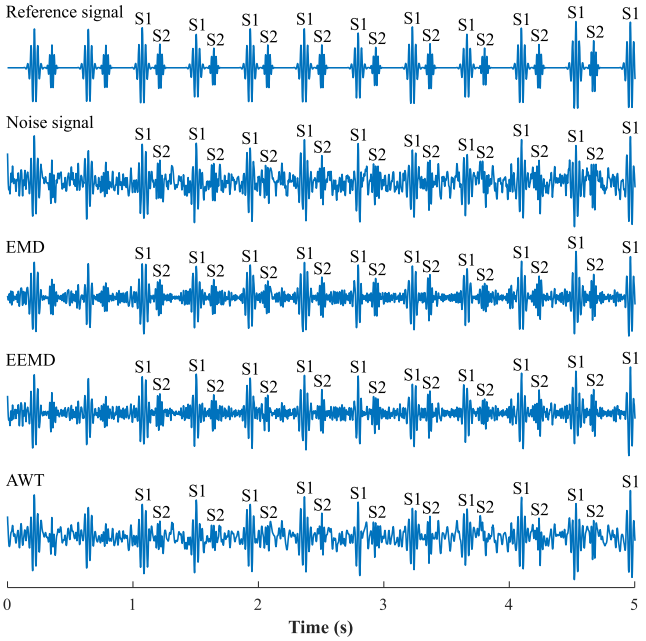

FIGURE 8. An example of the filtering movement artifacts of the mother and the fetus (the interference amplitude of 80.00) using all the methods tested.

prominent amplitude. In addition, it was able to filter out noise residues, thus the AWT approach is considered as the most effective when filtering the Gaussian noise. Similar performance characteristic of the methods was also observed when filtering the ambient noise.

Better results of the EMD and EEMD methods, based on the visual assessment, were achieved only for the interference caused by movement artifacts of the mother and the fetus. Fig. 8 shows an example of the filtering the movement artifacts (the interference amplitude of 80.00) using all the methods tested. Although very accurate fHR detection was achieved with all algorithms (considering the results of the statistical evaluation), higher SNR improvement was noticed for the EMD and EEMD methods when compared to the AWT approach. In terms of S1 sounds detection, low SNR improvement did not have any influence on the final AWT result, but in terms of S2 sounds detection, the AWT method would perform worse than the EMD and EEMD.

C. BLAND-ALTMAN PLOTS

Bland-Altman plots were used to graphically evaluate the quality of fHR determination using the EMD, EEMD and AWT methods. The verification outcome can be interpreted as follows: the smaller the range of the confidence interval, the smaller the difference between the fHR determined by the given method and the reference. Table 7 presents mean values of μ and values of $\pm 1.96\sigma$ for the methods tested and for all selected types (and levels) of interference. Based on these results it can be noticed that the EMD method was effective only in 4 out of 12, and the EEMD in 9 out of 12 considered cases. The best results were obtained using the AWT method, which was effective for all 12 cases, since all the resulting mean values of μ ranged from -1.00 to 1.00 bpm and, at the same time, the values of 1.96σ ranged from -5.00 to 5.00 bpm.

An example of Bland-Altman plots for the reference and estimated fHR values using the EMD method is shown in Fig. 9. Example a) presents the interference for which the EMD method was not effective (the ambient noise with the amplitude of 5.00), and example b) presents the interference for which high values of the quality measures were obtained (the movement artifacts with the amplitude of 30.00). Bland-Altman plots for the EEMD method are shown in Fig. 10. Example a) presents the interference for which the EEMD method achieved poor performance in determining the fHR (the Gaussian noise with the amplitude of 5.00), and example b) shows the interference for which highly accurate results were obtained (the movement artifacts with the amplitude of 30.00). An example of Bland-Altman plots when using the AWT method is shown in Fig. 11. The AWT method was highly effective in both presented cases, i.e., a) for the movement artifacts (amplitude of 100.00) and b) the ambient noise (amplitude of 1.00). With the movement artifacts the AWT method provided slightly worse results than for the fPCG signal disturbed by the ambient noise, however, the differences were negligible.

D. FETAL HEART RATE TRACES

The fHR traces were determined based on the moving averages and their accuracy was verified based on comparison to the reference recording. The graphical representation is inspired by FIGO classification [91]. Fig. 12 shows the comparison of reference and estimated fHR traces after filtering the ambient noise (the interference amplitude of 5.00) using

TABLE 7. Mean values of μ and values of $\pm 1.96\sigma$ for all methods when filtering ambient noise, Gaussian noise, and movement artifacts of the mother and the fetus.

Type of interference	Interference amplitude (-)	SNR of signal with noise (dB)	EMD		EEMD		AWT	
			μ (bpm)	$\pm 1.96\sigma$ (bpm)	μ (bpm)	$\pm 1.96\sigma$ (bpm)	μ (bpm)	$\pm 1.96\sigma$ (bpm)
Ambient noise	1.00	-1.16	0.01	0.03	0.08	0.08	-0.01	0.02
	1.50	-2.27	-1.15	3.39	0.02	0.11	-0.01	0.02
	2.50	-4.63	-1.55	5.81	0.01	0.85	0.02	0.11
	5.00	-9.36	-3.48	14.48	-2.48	5.66	-0.09	1.51
Gaussian noise	1.40	-2.12	-1.58	3.93	0.02	0.11	0.02	0.03
	2.00	-3.58	-1.20	4.36	0.03	0.14	0.02	0.11
	3.00	-5.89	-3.99	8.04	-0.19	1.59	0.06	0.20
	5.00	-9.55	-4.97	10.03	-4.01	8.40	-0.47	3.07
Movement artifacts	30.00	-0.50	0.01	0.03	0.01	0.06	0.01	0.06
	60.00	-1.74	-0.02	0.95	-0.15	1.36	0.03	0.95
	80.00	-2.73	-0.12	2.09	-0.78	3.39	0.02	1.27
	100.00	-3.74	-1.63	5.36	-2.14	5.89	-0.82	3.89

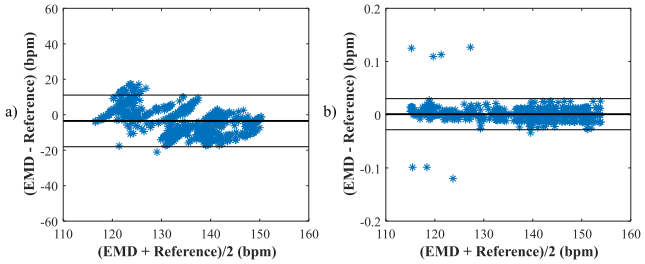

FIGURE 9. Comparison of reference and estimated fHR values using the EMD method obtained for the fPCG signal disturbed by: a) the ambient noise (amplitude of 5.00); and b) the movement artifacts (amplitude of 30.00).

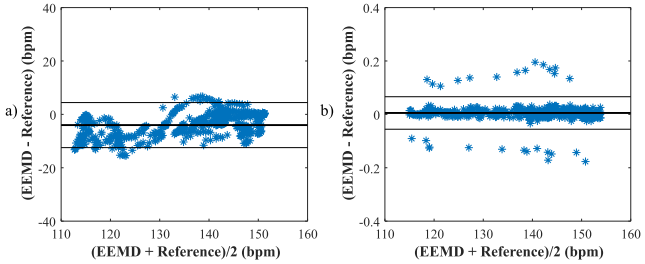

FIGURE 10. Comparison of reference and estimated fHR values using the EEMD method obtained for the fPCG signal disturbed by: a) the Gaussian noise (amplitude of 5.00); and b) the movement artifacts (amplitude of 30.00).

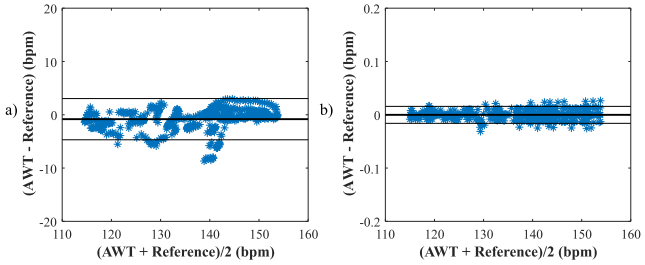

FIGURE 11. Comparison of reference and estimated fHR values using the AWT method obtained for the fPCG signal disturbed by: a) the movement artifacts (amplitude of 100.00); and b) the ambient noise (amplitude of 1.00).

all considered methods. Example a) presents a comparison of the fHR traces obtained using the EMD method, which provided poor results. It can be seen that the estimated EMD curve deviates from the reference one repeatedly. This means that the method does not work properly. Such deviations may affect the fHR determination and, subsequently, false diagnosis of fetal. Example b) presents a comparison of the fHR traces obtained using the EEMD method. In this case satisfactory results were achieved for a large part of the curve. The observed small deviations from the reference do not affect the accuracy of the fHR determination significantly. The EEMD method can, therefore, be considered as effective. Example c) presents a comparison of the fHR traces estimated with a help of the AWT method, which provided the best results. The AWT curve copies the reference trend over the entire signal length. This method can be considered as the most accurate and most suitable for the fHR determination from the fPCG signal disturbed by the ambient noise.

V. DISCUSSION

Based on the results presented in the previous chapter, it can be stated that accurate fHR determination from fPCG signals using advanced signal processing methods is possible. In this study, according to the statistical parameters, the worst results were obtained using the EMD method, which was effective in 7 out of 12 types and levels of interference, better results were obtained using the EEMD method, which was effective in 9 out of 12 kinds of interference, and the best results were achieved using the AWT method, which was effective for all considered noise types (and levels). According to the visual assessment, the most efficient detection of S1 sounds was achieved using the AWT method, when filtering the ambient and the Gaussian noise. While when filtering the movement artifacts of the mother and the fetus, there were no significant differences between the algorithms performance in terms of S1 sounds detection, but in terms of S2 sounds detection, the AWT method would perform worse than the EMD and EEMD.

It was also shown that for the low interference level, all the considered methods were able to filter the fPCG signal effectively and to determine the fHR accurately, despite the noise type. With a high interference amplitude, it was more

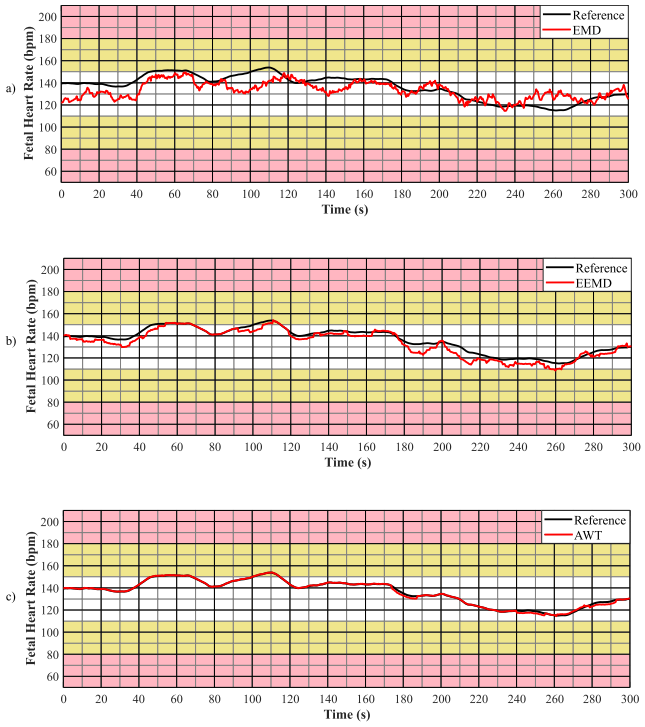

FIGURE 12. Comparison of reference and estimated fHR traces after filtering ambient noise (the interference amplitude of 5.00) extracted using: a) the EMD method (this method failed when filtering), b) the EEMD method (providing satisfactory results), and c) the AWT method, (highly accurate results).

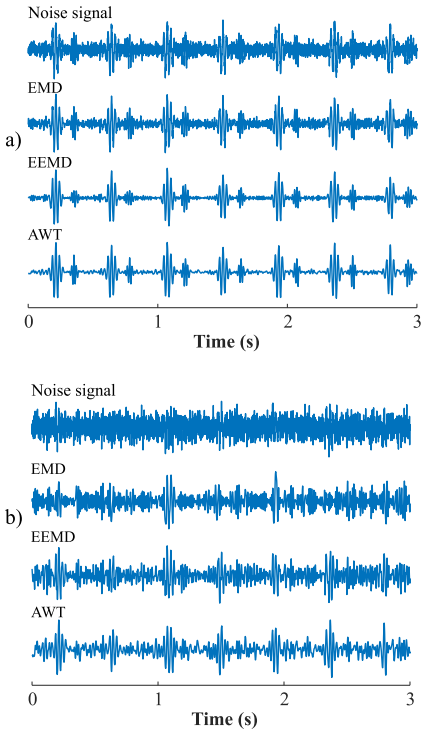

FIGURE 13. An example of the influence of the interference amplitude on the filtration results: a) the ambient noise of the amplitude 1.00, b) the ambient noise of the amplitude 5.00.

difficult for all the three methods to provide satisfactory filtering results. An example how the level of interference affects the filtration outcomes is shown in Fig. 13. Example a) presents the filtering of ambient noise of the amplitude equal to 1.00, while example b) concerns also the ambient noise, but of 5 times higher interference amplitude. It can be noticed that in the case of low level of interference, all the methods were able to filter the noise out properly. However, when a high level of interference was used, the EMD method failed in the filtration. The EEMD method achieved relatively good results, but still residual noise was present in the signal filtered. And the AWT approach was best able to filter out such a high level of noise. It can be concluded, that the quality of the fPCG recordings is very important factor for the subsequent signal processing. Due to the high level of interference and, thus, poorer filtration effectiveness, an important clinical information about the fetal condition can be lost. Especially the ambient noise (as door closing, speech, cough) could be rather easily eliminated while registering fPCG signals.

The resulting quality of the extracted signal and the accuracy of fHS detection are greatly influenced by the setting of the algorithm parameters. As an example, Fig. 14 shows the effect of different number of decomposition levels while keeping the same type and wavelength (*sym4*) for the AWT method. If only 1 (see Fig. 14a) or 2 (see Fig. 14b) decomposition levels were selected, the method failed to sufficiently suppress interference, which led to a reduction in the accuracy of S1 detection (ACC $<$ 94.00%). Contrary, when the number of decomposition levels was 3 (herein called ''optimal setting'', see Fig. 14c), all S1 echoes were detected (ACC $=$ 100.00%). Finally, using 4 decomposition levels (see Fig. 14d) can be considered unsuitable because, in addition to noise suppression, S1 echoes were slightly suppressed, and S2 echoes were completely suppressed, which would not allow their further analysis in the future. Further, Fig. 14 shows examples of signals extracted using 5 decomposition levels (Fig. 14e), 6 decomposition levels (Fig. 14f) 7 decomposition levels (Fig. 14g), and 8 decomposition levels (Fig. 14h). In all these cases, the decomposition level was too high, leading to disruption of the morphology of the fPCG signal, loss of important clinical information and low accuracy in the detection of fHSs. In all cases, ACC accuracy of $<$ 76.00% was achieved in the detection of S1 echoes, which has a significant effect on the accuracy of the fHR determination. Such inaccurate extraction could lead to a false positive diagnosis of fetal hypoxia.

Finally, we compared our results with those obtained in other studies. Objective comparison of results is challenging as there is a lack of open databases with reference annotations that accurately determine the position of fHSs. Thus, when testing fPCG extraction methods, different authors use various databases (*Shiraz University Fetal Heart Sounds Database* [14], [38], [82]) or use signals of their own [33], [37], [46], [81]. In addition, the signals obtain various interference of different types and intensities, and also use different evaluation techniques such as mean square error (MSE) [33] or software quality index (SQI) [81]. Some

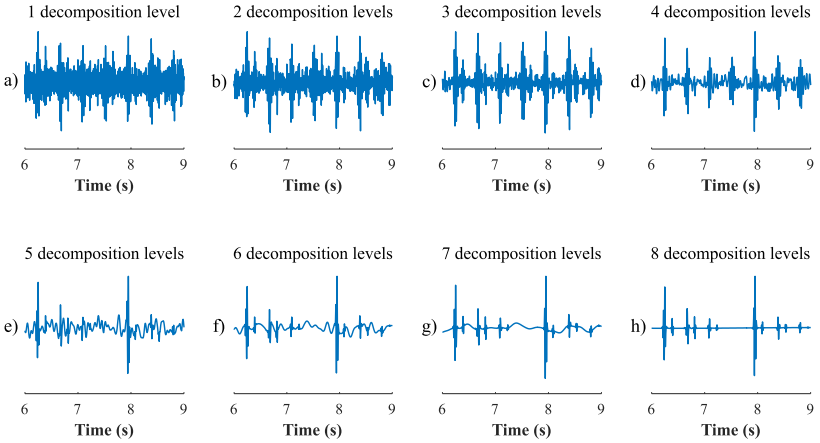

FIGURE 14. Influence of the number of decomposition levels on the quality of fPCG signal extraction. a) and b) low number of decomposition levels leading to insufficient noise suppression, c) optimal setting resulting in high quality fPCG extraction. d) inappropriate choice of decomposition levels suppressing S2 echoes; e), f), g) and h) demonstrate a high number of degradation levels leading to disruption in fPCG signal morphology and loss of clinical information.

TABLE 8. Comparison of the results with other studies.

Author, source	Algorithm	Dataset	S1 detection accuracy (%)	Advantages and limitations
Atteq et al. [14]	BSS methods	Real	–	+ effective separation of mHSs from fHSs - without statistical comparison
Jimenez-Gonzales et al. [12]	TDSEP	–		+ effective separation of mHSs from fHSs + large amplitude of extracted fHSs - without statistical comparison - low noise level filteringn
Koutsiana et al. [35]	WT-FD	Synthetic	60.00–100.00	+ tested also on pathological recordings - less effective at higher noise levels
Kovacs et al. [40]	AT-WT-MP	Real	92.90–98.50	+ tested at different noise levels + tested on signals with strong mHSs + tested on signals with significant S1 split + possible detection of murmurs - less effective at higher noise levels
Warbhe et al. [46]	EMD-SVD-EFICA	Real	–	+ clear identification of S1 and S2 fHSs - tested on a small number of recordings - low noise level filtering - without statistical comparison
Vaisman et al. [37]	AWT	Real	92.90–98.80	+ recordings from different noisy environments - less effective at higher noise levels
Samieinasab et al. [82]	EMD-NMF	Real	83.00–100.00	+ tested on a large number of recordings + tested also on recordings with abnormalities - less effective at higher noise levels
Taralunga et al. [64]	EMD	Synthetic	–	+ effective even for very noisy signals + robust method - without statistical comparison
Ruffo et al. [81]	MF-VBPF	Real	–	+ tested at different noise levels - less effective at higher noise levels
Proposed algorithms	EMD EEMD AWT	Synthetic	46.55–100.00 89.02–100.00 97.37–100.00	+ tested at different noise levels + AWT highly accurate even at higher noise levels + high SNR improvement + preservation of signal morphology - not tested on recordings with abnormalities

authors do not use any objective evaluation parameters and only evaluate the visual quality of the signals in time domain or [12], [46], [82] or their spectrograms [14], [43]. For these reasons, we made both objective and subjective comparison of the results summarized in Table 8.

- In [14] the authors tested BSS-based methods on real records. The authors did not present any statistical parameters, but according to the visual comparison, it can be argued that the methods were as effective as the methods proposed herein. In addition, they were able to effectively separate the maternal HSs (mHSs) and fHSs.
- The authors in [12] tested temporal decorrelation source separation (TDSEP) on real records with relatively low interference intensity. The resulting extracted signals

were not evaluated using statistical parameters. According to the visual evaluation, the method extracted fHSs with a sufficiently large magnitude an of a quality that is comparable to our methods.

- The combination of WT and fractal dimension was tested in [35] on two datasets with synthetic signals. Some signals were pathological and included cardiac arrhythmias. When detecting S1 echoes, an accuracy in the range of 60.00–100.00% was achieved, which is better results compared to the EMD method tested by us, but worse compared to EEMD and AWT.
- In [40], a combination of autocorrelation technique (AT), WT and matching pursuit (MP) methods was tested and evaluated on real records. The method was tested on recordings with low, medium and high noise levels, as well as on signals with strong mHSs or with significant S1 split. Accuracy in the range of 92.90–98.50% was achieved in the detection of echoes. These are better results compared to the EMD and EEMD methods presented by us, but worse results compared to the AWT method.
- The combination of ICA, SVD and EFICA was presented in [46]. The methods were tested on real records. Unfortunately, the authors do not present any statistical evaluation, they only show the waveforms of the extracted signals. According to the visual comparison, it can be stated that the filtration was comparably effective, but in their case, only lower levels of interference were filtered.
- The authors of the study presented in [37] tested the AWT method on real records. They achieved the best results using the *coiflet2*, 6 levels of decomposition and hard thresholding. The method was tested on records taken in quiet, noisy, mostly quiet, and mostly noisy environments. When evaluating the accuracy of the method, 92.90–98.80% was achieved, which means the method outperformed the EMD and EEMD tested herein but achieved worse results than the AWT method (with different settings) provided in our study.
- In [82], the authors combined EMD and nonnegative matrix factorization (NMF) and tested the performance of the algorithm on real records containing also signals with abnormalities. Accuracy of 83.00–100.00% was achieved. These are better results compared to the EMD method we tested, but worse compared to the EEMD and AWT methods.
- The EMD method was tested in [64] on synthetic signals. The authors do not present a statistical comparison of the results. According to the visual evaluation of the signals, it can be stated that the method achieved comparable results with the algorithms presented herein.
- The combination of matched filtering (MF) and variable band-pass filtering (VBPF) was tested in [82] on real records. The authors evaluated the performance of the algorithm according to different parameters, but according to the visual comparison it can be stated that the methods tested herein were able to suppress noise better, especially at the higher intensities, and also better emphasize S2 echoes.

This study proved that for effective filtration of fPCG signals, the filtration method and its optimal setting must be appropriately selected. Furthermore, when recording real fPCG signals, it is important to pay attention to the quality of the recordings, which significantly affects filtration efficiency. From a high-quality recording, it is possible to accurately determine the fHR and minimize the risk of misdiagnosis of the fetal hypoxia. Great number of publications focus on the adult PCG, which is different from the fetal one in many aspects (in both frequency and time domain). There are many specific interferences in fetal PCG that this study addresses. Currently, attention is paid to the area of fetal ECG, whereas the area of fetal PCG is still underdeveloped although it has great potential for home monitoring of the fetus.

The best results were achieved using the AWT, however, we have not tested the presence of the murmurs or any abnormal sounds, but it can be assumed that the algorithm will be able to perform well even on pathological records. The problem is lack of such recordings among the public databases. In fact, there is no publicly available database with fetal PCG with murmurs (only adults ones). This issue will be the subject of further research, we will work on collecting pathological data of our own, such as some authors did (such as Balogh, 2015 [92]). The aim is creating an open access database consisting of both pathological and physiological recordings that can be used for the evaluation of extraction and classification algorithms. The benefit of the article is the testing of methods that are known from other areas but have not yet been correctly tested in the field of fPCG processing. This is a pilot study in this area, research will continue, and other algorithms will be tested. According to Table 8, BSS-based methods, especially ICA, appear to be promising for the purpose of separating mHSs from fHSs. Adaptive algorithms (LMS or RLS), which can adapt to the changing nature of the signal, also have great potential. Hybrid algorithms will also be tested, which would combine the advantages of different methods.

VI. CONCLUSION

This study examined the effectiveness of advanced signal processing methods such as EMD, EEMD, and AWT used for the purpose of filtering fPCG signals. The main aim was to create a comprehensive and objective comparison of these methods when filtering three types of interference that are often recorded together with fPCG signals. Ambient noise, Gaussian noise, and movement artifacts of the mother and the fetus of various amplitudes were considered. The evaluation was performed by assessing the quality of S1 sounds detection and the ability to determine the fHR signal correctly. The effectiveness evaluation was performed using the statistical parameters (ACC, SE, PPV, and F1), the level of SNR increase, $\overline{|\Delta T_i|}$ values, the graphical outcome representation

with Bland-Altman plots and the visual assessment of the resulting fHR traces. Using the EMD method, ACC > 95% was achieved in 7 out of 12 considered types (and levels) of interference, with average ACC = 88.73%, SE = 91.57%, PPV = 94.80% and F1 = 93.12%. Based on the EEMD method, ACC > 95% was achieved in 9 out of 12 types (and levels) of noise, with average values of ACC = 97.49%, SE = 97.89%, PPV = 99.53% and F1 = 98.69%. Finally, with the AWT method, ACC > 95% was achieved in all 12 considered types (and levels) of interference, with average ACC = 99.34%, SE = 99.49%, PPV = 99.85% a F1 = 99.67%. In the light of these results, the AWT method proved to be the most suitable for filtering fPCG signals, however the EMD and EEMD procedures also demonstrated their effectiveness at lower interference amplitudes. The study showed that it is possible to achieve accurate S1 sound detection and to determine fHR correctly based on the advanced fPCG signal processing. The future work will concern the testing of methods on real fPCG recordings, as well as the ability to accurately detect S2 sounds.

REFERENCES

[1] R. Martinek, R. Kahankova, H. Nazeran, J. Konecny, J. Jezewski, P. Janku, P. Bilik, J. Zidek, J. Nedoma, and M. Fajkus, "Non-invasive fetal monitoring: A maternal surface ECG electrode placement-based novel approach for optimization of adaptive filter control parameters using the LMS and RLS algorithms," *Sensors*, vol. 17, no. 5, p. 1154, May 2017.

[2] M. Jezewski, R. Czabanski, K. Horoba, and J. Leski, "Clustering with pairs of prototypes to support automated assessment of the fetal state," *Appl. Artif. Intell.*, vol. 30, no. 6, pp. 572–589, Jul. 2016.

[3] M. Jezewski, R. Czabanski, and J. Leski, "An attempt to optimize the cardiotocographic signal feature set for fetal state assessment," *J. Med. Imag. Health Informat.*, vol. 5, no. 6, pp. 1364–1373, Nov. 2015.

[4] M. Jezewski, R. Czabanski, J. M. Leski, and J. Jezewski, "Fuzzy classifier based on clustering with pairs of ϵ-hyperballs and its application to support fetal state assessment," *Expert Syst. Appl.*, vol. 118, pp. 109–126, Mar. 2019.

[5] R. Czabanski, M. Jezewski, J. Wrobel, K. Horoba, and J. Jezewski, "A neuro-fuzzy approach to the classification of fetal cardiotocograms," in *Proc. 14th Nordic-Baltic Conf. Biomed. Eng. Med. Phys.*, vol. 20, R. Magjarevic, J. H. Nagel, A. Katashev, Y. Dekhtyar, and J. Spigulis, Eds. Berlin, Germany: Springer, 2008, pp. 446–449.

[6] R. Martinek, R. Kahankova, J. Jezewski, R. Jaros, J. Mohylova, M. Fajkus, J. Nedoma, P. Janku, and H. Nazeran, "Comparative effectiveness of ICA and PCA in extraction of fetal ECG from abdominal signals: Toward non-invasive fetal monitoring," *Frontiers Physiol.*, vol. 9, p. 648, May 2018.

[7] A. Matonia, J. Jezewski, K. Horoba, A. Gacek, and P. Labaj, "The maternal ECG suppression algorithm for efficient extraction of the fetal ECG from abdominal signal," in *Proc. Int. Conf. IEEE Eng. Med. Biol. Soc.*, Aug. 2006, pp. 3106–3109.

[8] M. J. Peters, J. G. Stinstra, S. Uzunbajakau, and N. Srinivasan, "Fetal magnetocardiography," in *Advances in Electromagnetic Fields in Living Systems*, vol. 4, J. C. Lin, Ed. New York, NY, USA: Springer, 2005, pp. 1–40.

[9] S. Strand, W. Lutter, J. F. Strasburger, V. Shah, O. Baffa, and R. T. Wakai, "Low-cost fetal magnetocardiography: A comparison of superconducting quantum interference device and optically pumped magnetometers," *J. Amer. Heart Assoc.*, vol. 8, no. 16, Aug. 2019, Art. no. e013436.

[10] M. Ladrova, M. Sidikova, R. Martinek, R. Jaros, and P. Bilik, "Elimination of interference in phonocardiogram signal based on wavelet transform and empirical mode decomposition," *IFAC-PapersOnLine*, vol. 52, no. 27, pp. 440–445, 2019.

[11] F. Kovacs and M. Torok, "An improved phonocardiographic method for fetal heart rate monitoring," in *Proc. 20th Annu. Int. Conf. IEEE Eng. Med. Biol. Soc., Biomed. Eng. Towards Year Beyond*, vol. 20, Nov. 1998, pp. 1719–1722.

[12] A. Jimenez-Gonzalez and C. J. James, "Source separation of foetal heart sounds and maternal activity from single-channel phonograms: A temporal independent component analysis approach," in *Proc. Comput. Cardiol.*, Sep. 2008, pp. 949–952.

[13] A. Sbrollini, A. Strazza, M. Caragiuli, C. Mozzoni, S. Tomassini, A. Agostinelli, M. Morettini, S. Fioretti, F. Di Nardo, and L. Burattini, "Fetal phonocardiogram denoising by wavelet transformation: Robustness to noise," in *Proc. Comput. Cardiol. Conf. (CinC)*, Sep. 2017, pp. 1–4.

[14] M. Atteeq, M. F. Khan, and A. N. Qureshi, "Fetus heart beat extraction from Mother's PCG using blind source separation," in *Proc. 11th Int. Conf. Bioinf. Biomed. Technol.*, May 2019, pp. 100–104.

[15] P. C. Adithya, R. Sankar, W. A. Moreno, and S. Hart, "Trends in fetal monitoring through phonocardiography: Challenges and future directions," *Biomed. Signal Process. Control*, vol. 33, pp. 289–305, Mar. 2017.

[16] M. Cesarelli, M. Ruffo, M. Romano, and P. Bifulco, "Simulation of foetal phonocardiographic recordings for testing of FHR extraction algorithms," *Comput. Methods Programs Biomed.*, vol. 107, no. 3, pp. 513–523, Sep. 2012.

[17] M. Ruffo, "Foetal heart rate recording: Analysis and comparison of different methodologies," Ph.D. dissertation, Alma, 2011. [Online]. Available: http://amsdottorato.unibo.it/3345/, doi: 10.6092/unibo/amsdottorato/3345.

[18] Q.-U.-A. Mubarak, M. U. Akram, A. Shaukat, F. Hussain, S. G. Khawaja, and W. H. Butt, "Analysis of PCG signals using quality assessment and homomorphic filters for localization and classification of heart sounds," *Comput. Methods Programs Biomed.*, vol. 164, pp. 143–157, Oct. 2018.

[19] E. Kennedy, *Observations on Obstetric Auscultation: With an Analysis of the Evidences of Pregnancy, and an Inquiry Into the Proofs of the Life and Death of the Foetus in Utero*. London, U.K.: J. & HG Langley, 1833.

[20] R. K. Freeman, T. J. Garite, M. P. Nageotte, and L. A. Miller, *Fetal Heart Rate Monitoring*. Philadelphia, PA, USA: Lippincott Williams & Wilkins, 2012.

[21] F. Kovács, C. Horváth, A. T. Balogh, and G. Hosszú, "Fetal phonocardiography—Past and future possibilities," *Comput. Methods Programs Biomed.*, vol. 104, no. 1, pp. 19–25, Oct. 2011.

[22] S. Leng, R. S. Tan, K. T. C. Chai, C. Wang, D. Ghista, and L. Zhong, "The electronic stethoscope," *Biomed. Eng. OnLine*, vol. 14, no. 1, p. 66, Dec. 2015.

[23] M. Anumukonda and S. R. Chowdhury, "Heart sound sensing through MEMS microphone," in *Sensors for Everyday Life*, vol. 22, O. A. Postolache, S. C. Mukhopadhyay, K. P. Jayasundera, and A. K. Swain, Eds. Cham, Switzerland: Springer, 2017, pp. 121–134.

[24] K. Yang, H. Jiang, J. Dong, C. Zhang, and Z. Wang, "An adaptive real-time method for fetal heart rate extraction based on phonocardiography," in *Proc. IEEE Biomed. Circuits Syst. Conf. (BioCAS)*, Nov. 2012, pp. 356–359.

[25] A. J. Zuckerwar, R. A. Pretlow, J. W. Stoughton, and D. A. Baker, "Development of a piezopolymer pressure sensor for a portable fetal heart rate monitor," *IEEE Trans. Biomed. Eng.*, vol. 40, no. 9, pp. 963–969, Sep. 1993.

[26] A. K. Mittra and N. K. Choudhari, "Development of a low cost fetal heart sound monitoring system for home care application," *J. Biomed. Sci. Eng.*, vol. 02, no. 06, pp. 380–389, 2009.

[27] A. Khandoker, E. Ibrahim, S. Oshio, and Y. Kimura, "Validation of beat by beat fetal heart signals acquired from four-channel fetal phonocardiogram with fetal electrocardiogram in healthy late pregnancy," *Sci. Rep.*, vol. 8, no. 1, Dec. 2018, Art. no. 13635.

[28] H. G. Goovaerts, H. P. van Geijn, and O. Rompelman, "An inductive sensor for recording of fetal movements and sounds," in *Proc. Annu. Int. Conf. IEEE Eng. Med. Biol. Soc.*, vol. 13, Nov. 1991, pp. 1622–1623.

[29] R. Martinek, J. Nedoma, M. Fajkus, R. Kahankova, J. Konecny, P. Janku, S. Kepak, P. Bilik, and H. Nazeran, "A phonocardiographic-based fiber-optic sensor and adaptive filtering system for noninvasive continuous fetal heart rate monitoring," *Sensors*, vol. 17, no. 4, p. 890, Apr. 2017.

[30] P. Várady, L. Wildt, Z. Benyó, and A. Hein, "An advanced method in fetal phonocardiography," *Comput. Methods Programs Biomed.*, vol. 71, no. 3, pp. 283–296, Jul. 2003.

[31] M. Moghavvemi, B. H. Tan, and S. Y. Tan, "A non-invasive PC-based measurement of fetal phonocardiography," *Sens. Actuators A, Phys.*, vol. 107, no. 1, pp. 96–103, Oct. 2003.

[32] J. Chen, K. Phua, Y. Song, and L. Shue, "A portable phonocardiographic fetal heart rate monitor," in *Proc. IEEE Int. Symp. Circuits Syst.*, May 2006, p. 4.

[33] V. S. Chourasia and A. K. Tiwari, "Design methodology of a new wavelet basis function for fetal phonocardiographic signals," *Sci. World J.*, vol. 2013, pp. 1–12, Apr. 2013.

[34] R. Jaros, R. Martinek, R. Kahankova, J. Vanus, M. Fajkus, and J. Nedoma, "Comparison of fetal phonocardiography de-noising by wavelet transform and the FIR filter," in *Proc. IEEE 20th Int. Conf. e-Health Netw., Appl. Services (Healthcom)*, Sep. 2018, pp. 1–5.
[35] E. Koutsiana, L. J. Hadjileontiadis, I. Chouvarda, and A. H. Khandoker, "Fetal heart sounds detection using wavelet transform and fractal dimension," *Frontiers Bioeng. Biotechnol.*, vol. 5, p. 49, Sep. 2017.
[36] S. R. Messer, J. Agzarian, and D. Abbott, "Optimal wavelet denoising for phonocardiograms," *Microelectron. J.*, vol. 32, no. 12, pp. 931–941, Dec. 2001.
[37] S. Vaisman, S. Y. Salem, G. Holcberg, and A. B. Geva, "Passive fetal monitoring by adaptive wavelet denoising method," *Comput. Biol. Med.*, vol. 42, no. 2, pp. 171–179, Feb. 2012.
[38] S. Tomassini, A. Strazza, A. Sbrollini, I. Marcantoni, M. Morettini, S. Fioretti, and L. Burattini, "Wavelet filtering of fetal phonocardiography: A comparative analysis," *Math. Biosci. Eng.*, vol. 16, no. 5, pp. 6034–6046, 2019.
[39] P. Varady, "Wavelet-based adaptive denoising of phonocardiographic records," in *Proc. Conf. Proc. 23rd Annu. Int. Conf. IEEE Eng. Med. Biol. Soc.*, Oct. 2001, pp. 1846–1849.
[40] F. Kovacs, C. Horváth, Á. T. Balogh, and G. Hosszú, "Extended non-invasive fetal monitoring by detailed analysis of data measured with phonocardiography," *IEEE Trans. Biomed. Eng.*, vol. 58, no. 1, pp. 64–70, Jan. 2011.
[41] A. Gavrovska, M. Slavkovic, I. Reljin, and B. Reljin, "Application of wavelet and EMD-based denoising to phonocardiograms," in *Proc. Int. Symp. Signals, Circuits Syst. ISSCS*, Jul. 2013, pp. 1–4.
[42] A. Cheema and M. Singh, "An application of phonocardiography signals for psychological stress detection using non-linear entropy based features in empirical mode decomposition domain," *Appl. Soft Comput.*, vol. 77, pp. 24–33, Apr. 2019.
[43] D. S. V. Sankar and L. P. Roy, "Principal component analysis (PCA) approach to segment primary components from pathological phonocardiogram," in *Proc. Int. Conf. Commun. Signal Process.*, Apr. 2014, pp. 910–914.
[44] R. Jaros, R. Kahankova, R. Martinek, J. Nedoma, M. Fajkus, and Z. Slanina, "Fetal phonocardiography signal processing from abdominal records by non-adaptive methods," in *Photonics Applications in Astronomy, Communications, Industry, and High-Energy Physics Experiments*, R. S. Romaniuk and M. Linczuk, Eds. Wilga, Poland: SPIE, Oct. 2018, p. 118.
[45] M. R. Potdar, D. M. Meshram, N. Dewangan, and D. R. Kumar, "Implementation of adaptive algorithm for PCG signal denoising," *IJIREEICE*, vol. 3, no. 4, pp. 33–42, Apr. 2015.
[46] A. D. Warbhe, R. V. Dharaskar, and B. Kalambhe, "A single channel phonocardiograph processing using EMD, SVD, and EFICA," in *Proc. 3rd Int. Conf. Emerg. Trends Eng. Technol.*, Nov. 2010, pp. 578–581.
[47] T. Chakrabarti, S. Saha, S. Roy, and I. Chel, "Phonocardiogram signal analysis–practices, trends and challenges: A critical review," in *Proc. Int. Conf. Workshop Comput. Commun. (IEMCON)*, Oct. 2015, pp. 1–4.
[48] V. K. Shivhare, S. N. Sharma, and D. K. Shakya, "Detection of heart sounds s1 and s2 using optimized S-transform and back—Propagation algorithm," in *Proc. IEEE Bombay Sect. Symp. (IBSS)*, Sep. 2015, pp. 1–6.
[49] S. E. Schmidt, C. Holst-Hansen, C. Graff, E. Toft, and J. J. Struijk, "Segmentation of heart sound recordings by a duration-dependent hidden Markov model," *Physiological Meas.*, vol. 31, no. 4, pp. 513–529, Apr. 2010.
[50] D. Springer, L. Tarassenko, and G. Clifford, "Logistic regression-HSMM-based heart sound segmentation," *IEEE Trans. Biomed. Eng.*, vol. 63, no. 4, pp. 822–832, Apr. 2016.
[51] X. Quan, J. Seok, and K. Bae, "Detection of S1/S2 components with extraction of murmurs from phonocardiogram," *IEICE Trans. Inf. Syst.*, vol. E98.D, no. 3, pp. 745–748, 2015.
[52] V. Nivitha Varghees and K. I. Ramachandran, "Heart murmur detection and classification using wavelet transform and Hilbert phase envelope," in *Proc. 21st Nat. Conf. Commun. (NCC)*, Feb. 2015, pp. 1–6.
[53] C. D. Papadaniil and L. J. Hadjileontiadis, "Efficient heart sound segmentation and extraction using ensemble empirical mode decomposition and kurtosis features," *IEEE J. Biomed. Health Informat.*, vol. 18, no. 4, pp. 1138–1152, Jul. 2014.
[54] F. Chakir, A. Jilbab, C. Nacir, A. Hammouch, and A. Hajjam El Hassani, "Detection and identification algorithm of the s1 and s2 heart sounds," in *Proc. Int. Conf. Electr. Inf. Technol. (ICEIT)*, May 2016, pp. 418–420.
[55] E. F. Gomes, P. Bentley, M. Coimbra, E. Pereira, and Y. Deng, "Classifying heart sounds—Approaches to the PASCAL challenge," in *Proc. Int. Conf. Health Inform.*, Barcelona, Spain: SciTePress, 2013, pp. 337–340.
[56] S. D. Min and H. Shin, "A localization method for first and second heart sounds based on energy detection and interval regulation," *J. Electr. Eng. Technol.*, vol. 10, no. 5, pp. 2126–2134, Sep. 2015.
[57] V. S. Chourasia, A. K. Tiwari, and R. Gangopadhyay, "A novel approach for phonocardiographic signals processing to make possible fetal heart rate evaluations," *Digit. Signal Process.*, vol. 30, pp. 165–183, Jul. 2014.
[58] A. Strazza, A. Sbrollini, V. di Battista, R. Ricci, L. Trillini, I. Marcantoni, M. Morettini, S. Fioretti, and L. Burattini, "PCG-delineator: An efficient algorithm for automatic heart sounds detection in fetal phonocardiography," in *Proc. Comput. Cardiol. Conf. (CinC)*, Dec. 2018, pp. 1–4.
[59] M. Romano, G. Faiella, F. Clemente, L. Iuppariello, P. Bifulco, and M. Cesarelli, "Analysis of foetal heart rate variability components by means of empirical mode decomposition," in *Proc. 15th Medit. Conf. Med. Biol. Eng. Comput.*, vol. 57, E. Kyriacou, S. Christofides, and C. S. Pattichis, Eds. Cham, Switzerland: Springer, 2016, pp. 71–74.
[60] H. Ahmadi and A. Ekhlasi, "Types of EMD algorithms," in *Proc. 5th Iranian Conf. Signal Process. Intell. Syst. (ICSPIS)*, Dec. 2019, pp. 1–5.
[61] A.-O. Boudraa and J.-C. Cexus, "EMD-based signal filtering," *IEEE Trans. Instrum. Meas.*, vol. 56, no. 6, pp. 2196–2202, Dec. 2007.
[62] A. Zeiler, R. Faltermeier, I. R. Keck, A. M. Tome, C. G. Puntonet, and E. W. Lang, "Empirical mode decomposition—An introduction," in *Proc. Int. Joint Conf. Neural Netw. (IJCNN)*, Barcelona, Spain, Jul. 2010, pp. 1–8.
[63] H. Chaudhari, S. L. Nalbalwar, and R. Sheth, "A review on intrensic mode function of EMD," in *Proc. Int. Conf. Electr., Electron., Optim. Techn. (ICEEOT)*, Mar. 2016, pp. 2349–2352.
[64] D. D. Taralunga, M. Ungureanu, B. Hurezeanu, and R. Strungaru, "Fetal heart rate estimation from phonocardiograms using an EMD based method," in *Proc. 19th Int. Conf. Comput., Recent Adv., Comput. Sci.*, 2015, pp. 414–417.
[65] J. Lin, "Improved ensemble empirical mode decomposition method and its simulation," in *Advances in Intelligent Systems*, vol. 138, G. Lee, Ed. Berlin, Germany: Springer, 2012, pp. 109–115.
[66] S. Gaci, "A new ensemble empirical mode decomposition (EEMD) denoising method for seismic signals," *Energy Procedia*, vol. 97, pp. 84–91, Nov. 2016.
[67] P. K. Ghosh and D. Poonia, "Comparison of some EMD based technique for baseline wander correction in fetal ECG signa," *Int. J. Comput. Appl.*, vol. 116, no. 15, pp. 48–52, Apr. 2015.
[68] Z. Wu and N. E. Huang, "Ensemble empirical mode decomposition: A noise-assisted data analysis method," *Adv. Adapt. Data Anal.*, vol. 1, no. 1, pp. 1–41, Jan. 2009.
[69] M. E. Torres, M. A. Colominas, G. Schlotthauer, and P. Flandrin, "A complete ensemble empirical mode decomposition with adaptive noise," in *Proc. IEEE Int. Conf. Acoust., Speech Signal Process. (ICASSP)*, May 2011, pp. 4144–4147.
[70] D. D. Taralunga and G. M. Neagu, "An ensemble empirical mode decomposition based method for fetal phonocardiogram enhancement," in *World Congress on Medical Physics and Biomedical Engineering*, vols. 2–68, L. Lhotska, L. Sukupova, I. Lacković, and G. S. Ibbott, Eds. Singapore: Springer, 2019, pp. 387–391.
[71] J. A. Jimenez, M. A. Becerra, and E. Delgado-Trejos, "Heart murmur detection using ensemble empirical mode decomposition and derivations of the mel-frequency cepstral coefficients on 4-area phonocardiographic signals," in *Proc. Comput. Cardiol.*, Sep. 2014, pp. 493–496.
[72] P. M. Bentley and J. T. E. McDonnell, "Wavelet transforms: An introduction," *Electron. Commun. Eng. J.*, vol. 6, no. 4, pp. 175–186, Aug. 1994.
[73] D. Valencia, D. Orejuela, J. Salazar, and J. Valencia, "Comparison analysis between rigrsure, sqtwolog, heursure and minimaxi techniques using hard and soft thresholding methods," in *Proc. 21st Symp. Signal Process., Images Artif. Vis. (STSIVA)*, Aug. 2016, pp. 1–5.
[74] P. K. Jain and A. K. Tiwari, "An adaptive thresholding method for the wavelet based denoising of phonocardiogram signal," *Biomed. Signal Process. Control*, vol. 38, pp. 388–399, Sep. 2017.
[75] F. Arab, S. M. Daud, and S. Z. Hashim, "Discrete wavelet transform domain techniques," in *Proc. Int. Conf. Informat. Creative Multimedia*, Sep. 2013, pp. 340–345.
[76] J. S. Kulkarni, "Wavelet transform applications," in *Proc. 3rd Int. Conf. Electron. Comput. Technol.*, Kanyakumari, India, Apr. 2011, pp. 11–17.
[77] I. Daubechies, "The wavelet transform, time-frequency localization and signal analysis," *IEEE Trans. Inf. Theory*, vol. 36, no. 5, pp. 961–1005, Sep. 1990.

[78] O. Rioul and M. Vetterli, "Wavelets and signal processing," *IEEE Signal Process. Mag.*, vol. 8, no. 4, pp. 14–38, Oct. 1991.
[79] J. Rafiee, M. A. Rafiee, N. Prause, and M. P. Schoen, "Wavelet basis functions in biomedical signal processing," *Expert Syst. Appl.*, vol. 38, no. 5, pp. 6190–6201, May 2011.
[80] A. L. Goldberger, L. A. N. Amaral, L. Glass, J. M. Hausdorff, P. C. Ivanov, R. G. Mark, J. E. Mietus, G. B. Moody, C.-K. Peng, and H. E. Stanley, "PhysioBank, PhysioToolkit, and PhysioNet: Components of a new research resource for complex physiologic signals," *Circulation*, vol. 101, no. 23, Jun. 2000.
[81] M. Ruffo, M. Cesarelli, M. Romano, P. Bifulco, and A. Fratini, "An algorithm for FHR estimation from foetal phonocardiographic signals," *Biomed. Signal Process. Control*, vol. 5, no. 2, pp. 131–141, Apr. 2010.
[82] M. Samieinasab and R. Sameni, "Fetal phonocardiogram extraction using single channel blind source separation," in *Proc. 23rd Iranian Conf. Electr. Eng.*, May 2015, pp. 78–83.
[83] R. Martinek, R. Jaros, R. Kahankova, and K. Barnova, "Synthetic fetal PCG signals," *IEEE Access*, Nov. 2020. [Online]. Available: https://ieee-dataport.org/documents/synthetic-fetal-pcg-signals, doi: 10.21227/tgvb-rw67.
[84] C. Liu, D. Springer, Q. Li, B. Moody, R. A. Juan, F. J. Chorro, F. Castells, J. M. Roig, I. Silva, A. E. Johnson, and Z. Syed, "An open access database for the evaluation of heart sound algorithms," *Physiolog. Meas.*, vol. 37, no. 12, pp. 2181–2213, Dec. 2016. [Online]. Available: https://iopscience.iop.org/article/10.1088/0967-3334/37/12/2181
[85] J. Pan and W. J. Tompkins, "A real-time QRS detection algorithm," *IEEE Trans. Biomed. Eng.*, vol. BME-32, no. 3, pp. 230–236, Mar. 1985.
[86] L. Sathyapriya, L. Murali, and T. Manigandan, "Analysis and detection R-peak detection using modified pan-tompkins algorithm," in *Proc. IEEE Int. Conf. Adv. Commun., Control Comput. Technol.*, May 2014, pp. 483–487.
[87] A. Agostinelli, I. Marcantoni, E. Moretti, A. Sbrollini, S. Fioretti, F. Di Nardo, and L. Burattini, "Noninvasive fetal electrocardiography—Part I: Pan-Tompkins' algorithm adaptation to fetal R-peak identification," *Open Biomed. Eng. J.*, vol. 11, no. 1, pp. 17–24, Mar. 2017.
[88] L. Billeci and M. Varanini, "A combined independent source separation and quality index optimization method for fetal ECG extraction from abdominal maternal leads," *Sensors*, vol. 17, no. 5, p. 1135, May 2017.
[89] J. M. Bland and D. G. Altman, "Measuring agreement in method comparison studies," *Stat. Methods Med. Res.*, vol. 8, no. 2, pp. 135–160, Jun. 1999.
[90] T. Kupka, A. Matonia, M. Jezewski, J. Jezewski, K. Horoba, J. Wrobel, R. Czabanski, and R. Martinek, "New method for beat-to-beat fetal heart rate measurement using Doppler ultrasound signal," *Sensors*, vol. 20, no. 15, p. 4079, Jul. 2020.
[91] T. Kazmi, F. Radfer, and S. Khan, "ST analysis of the fetal ECG, as an adjunct to fetal heart rate monitoring in labour: A review," *Oman Med. J.*, vol. 26, no. 6, pp. 459–460, Nov. 2011.
[92] A. T. Balogh, "Analysis of the heart sounds and murmurs of fetuses and preterm infants," Ph.D. dissertation, Pázmány Péter Katolikus Egyetem, Budapest, Hungary, 2015.

RADEK MARTINEK (Member, IEEE) was born in Czech Republic, in 1984. He received the master's degree in information and communication technology from the VSB–Technical University of Ostrava, in 2009. Since 2012, he has been working as a Research Fellow. In 2014, he successfully defended his dissertation thesis titled The Use of Complex Adaptive Methods of Signal Processing for Refining the Diagnostic Quality of the Abdominal Fetal Electrocardiogram. He has become an Associate Professor in Technical Cybernetics in 2017 after defending the habilitation thesis titled Design and Optimization of Adaptive Systems for Applications of Technical Cybernetics and Biomedical Engineering Based on Virtual Instrumentation. He has been working as an Associate Professor with the VSB–Technical University of Ostrava since 2017. His current research interests include digital signal processing (linear and adaptive filtering, soft computing-artificial intelligence and adaptive fuzzy systems, non-adaptive methods, biological signal processing, and digital processing of speech signals), wireless communications (software-defined radio), and power quality improvement. He has more than 200 journal and conference articles in his research areas.

KATERINA BARNOVA was born in Ostrava, Czech Republic, in 1993. She received the master's degree from the Department of Cybernetics and Biomedical Engineering, VSB–Technical University of Ostrava, in 2019, where she is currently pursuing the Ph.D. degree in technical cybernetics. Her research interest includes advanced signal processing methods, especially for fECG extraction.

RENE JAROS was born in Ostrava, Czech Republic, in 1992. He received the bachelor's degree and the master's degree in biomedical engineering from the Department of Cybernetics and Biomedical Engineering, VSB–Technical University of Ostrava, in 2015 and 2017, respectively, and the Ph.D. degree in technical cybernetics, in 2019. His research interest includes fECG extraction by using hybrid methods.

RADANA KAHANKOVA was born in Opava, Czech Republic, in 1991. She received the bachelor's degree and the master's degree in biomedical engineering from the Department of Cybernetics and Biomedical Engineering, VSB–Technical University of Ostrava, in 2014 and 2016, respectively, and the Ph.D. degree in technical cybernetics, in 2019. Her current research interest includes improving the quality of electronic fetal monitoring.

TOMASZ KUPKA was born in Poland, in 1975. He received the M.Sc. degree in electronic engineering and the Ph.D. degree in biocybernetics and biomedical engineering from the Silesian University of Technology, Gliwice, Poland, in 2000 and 2018, respectively. He is currently a Project Leader with the Biomedical Signal Processing Department, Łukasiewicz Research Network, Institute of Medical Technology and Equipment, Zabrze, Poland. His research interests include fetal electrocardiography, electrohysterography, cardiotocography based on the Doppler ultrasound signal, mobile biomedical instrumentations, and software development for computerized fetal monitoring systems. He is a member of the Polish Society of Biomedical Engineering.

MICHAL JEZEWSKI was born in 1982 in Zabrze, Poland. He received the M.Sc. degree in computer science and the Ph.D. degree in electronics from the Silesian University of Technology, Gliwice, Poland, in 2006 and 2011, respectively. He is currently with the Department of Cybernetics, Nanotechnology, and Data Processing, Silesian University of Technology. His research interests include biomedical signal processing, computational intelligence methods with emphasis on fuzzy clustering, and fuzzy classifiers. He is a member of the Polish Society of Theoretical and Applied Electrotechnics.

ROBERT CZABANSKI was born in Tychy, Poland. He received the M.Sc. and Ph.D. degrees in electronics and the D.Sc. degree in biocybernetics and biomedical engineering from the Silesian University of Technology, Gliwice, Poland, in1997, 2003, and 2018, respectively. He is currently with the Department of Cybernetics, Nanotechnology, and Data Processing, Silesian University of Technology. His research interests include fuzzy and neuro-fuzzy modeling, learning theory, and biomedical signal processing. He is a member of the Polish Society of Theoretical and Applied Electrotechnics.

ADAM MATONIA was born in Poland, in 1975. He received the M.Sc. degree in electronic engineering and the Ph.D. degree in biocybernetics and biomedical engineering from the Silesian University of Technology, Gliwice, Poland, in 2000 and 2018, respectively. He is currently a Project Leader with the Biomedical Signal Processing Department, Łukasiewicz Research Network, Institute of Medical Technology and Equipment, Zabrze, Poland. His research interests include fetal electrocardiography, electrohysterography, mobile biomedical instrumentations, and the software development for computerized fetal monitoring systems. He is a member of the Polish Society of Biomedical Engineering. He was a Fellowship holder of the Foundation for Polish Science in 2005.

JANUSZ JEZEWSKI (Senior Member, IEEE) was born in Zabrze, Poland. He received the M.Sc. degree in electronics from the Silesian University of Technology, Gliwice, Poland, the Ph.D. degree in biological sciences from the University of Medical Sciences, Poznan, Poland, and the D.Sc. degree in biocybernetics and biomedical engineering from the Institute of Biocybernetics and Biomedical Engineering,Polish Academy of Sciences, Warsaw, Poland. He received the title of Professor conferred from the President of the Republic of Poland. He is currently a Director of science of the Łukasiewicz Research Network, Institute of Medical Technology and Equipment, Zabrze. He has authored or coauthored more than 300 international journal and conference papers. His research interests include biomedical instrumentation, digital signal processing, and application of computational intelligence in medical cyber-physical systems. He is a member of the Committee of Biocybernetics and Biomedical Engineering of the Polish Academy of Sciences, the Polish Society of Biomedical Engineering, the Institute of Physics and Engineering in Medicine, and the European Society for Engineering and Medicine.

KRZYSZTOF HOROBA was born in Poland, in 1968. He received M.S. degree in electronic engineering from the Silesian University of Technology, Gliwice, Poland, in 1993, the Ph.D. degree in medical science from the University of Medical Sciences, Poznan, Poland, in 2001, and the D.Sc. degree in biocybernetics and biomedical engineering from the Silesian University of Technology, in 2017. He is currently the Head of the Biomedical Signals Processing Department, Łukasiewicz Research Network, Institute of Medical Technology and Equipment, Zabrze, Poland. His research interests include fetal electrocardiography and electrohysterography, as well as the software development of the computerized fetal monitoring systems. He is a member of the Polish Society of Biomedical Engineering. He was a Fellowship holder of the Foundation for Polish Science in 1997.